

# Charge-transfer bonding in metal–arene coordination

Stephan M. Hubig, Sergey V. Lindeman, Jay K. Kochi \*

*Department of Chemistry, University of Houston, Houston, TX 77204-5641, USA*

Received 23 September 1999; accepted 23 February 2000

## Contents

|   |     |
|---|-----|
| Abstract . . . . .  | 831 |
| 1. Introduction . . . . .   | 832 |
| 2. Effects of charge transfer on the structure of metal–arene complexes . . . . .   | 834 |
| 2.1 Expansion of the arene ring . . . . .   | 834 |
| 2.2 $\pi$ -Bond localization in the arene ring . . . . .                            | 837 |
| 2.3 Loss of planarity of the arene ring . . . . .                                   | 840 |
| 2.4 The metal–arene bonding distance . . . . .                                      | 842 |
| 2.5 Change of donor–acceptor properties of metal-coordinated arene ligands. . . . . | 844 |
| 3. Charge-transfer activation of metal-coordinated arene ligands. . . . .           | 845 |
| 3.1 Carbon–hydrogen bond activation . . . . .                                       | 846 |
| 3.2 Nucleophilic–electrophilic <i>umpolung</i> . . . . .                            | 853 |
| 4. $\eta^1$ - and $\eta^2$ -Coordinated arene ligands . . . . .                     | 856 |
| 5. Conclusions. . . . .   | 869 |
| Acknowledgements . . . . .  | 869 |
| References . . . . .  | 869 |

## Abstract

X-ray crystallographic structures of donor–acceptor complexes of aromatic hydrocarbons with transition metals are re-examined with the focus on the arene ligands. Thus, significant structural and electronic changes are revealed in the arene moiety due to coordination to the metal center including: (i) expansion of the aromatic six-carbon ring; (ii) endocyclic  $\pi$ -bond localization; (iii) distortion of the planarity (folding) of the arene ring; and (iv) shortening of the metal–arene bond distances. All structural features are characteristic of metal–arene ( $\pi$ -

\* Corresponding author. Tel.: +1-713-7433290; fax: +1-713-7432709.

*E-mail address:* jkochi@pop.uh.edu (J.K. Kochi).

or  $\sigma$ -) complexes that exhibit various degrees of (metal-to-ligand) charge transfer. The concept of charge-transfer bonding not only explains the structural details but also the various facets of chemical reactivity of metal-coordinated arenes including efficient carbon–hydrogen bond activation and nucleophilic–electrophilic *umpolung*, both of which are critical factors in homogeneous metal catalysis. © 2000 Elsevier Science S.A. All rights reserved.

**Keywords:** Metal–arene coordination; Donor–acceptor complex; Charge-transfer bonding; Electrophilic–nucleophilic *umpolung*; C–H bond activation; X-ray structures

---

## 1. Introduction

Arenes represent one of the most important classes of  $\pi$ -ligands in organometallic chemistry. Owing to their ability to provide up to six electrons for coordination, numerous donor–acceptor complexes of various hapticities ( $\eta^1$  through  $\eta^6$ ) are known between arene ligands and metal centers, many of which have been identified as crucial intermediates in homogeneous metal catalysis [1–5] of various aromatic reactions. It is well known that arenes undergo substantial changes in reactivity upon coordination to a metal center — the two most important chemical effects include efficient carbon–hydrogen bond activation and nucleophilic–electrophilic *umpolung* of the arene reactivity. The favorable energetics of C–H bond activation of metal-coordinated arenes is exploited in organometallic catalysis, and the facile attack of metal–arene complexes by nucleophiles is extensively utilized to functionalize arenes (*vide infra*). Thus, the question arises as to the structural and electronic origin of such substantial changes in the reactivity of arenes in organometallic complexes.

X-ray crystallographic studies of metal–arene complexes generally focus on the metal center and the symmetry of its orbitals in the ligand environment. However, the structural details of the arene ligand, which are relevant for understanding its reactivity, are rarely discussed and often completely ignored. In this review, we take an alternative approach and examine metal–arene bonding from the viewpoint of the aromatic ligand. Thus, we provide a careful re-evaluation of X-ray crystallographic data of metal–arene complexes with the focus on the frequently subtle and often unnoticed structural changes in the arene ligands due to coordination to a metal center. The structural changes include ring expansion, endocyclic  $\pi$ -bond localization, and distortion of the planarity of the arene ring which (separately or all together) ultimately lead to a complete loss of the aromaticity of the  $\pi$ -system. These structural features all point to strong electronic interactions between arene and metal center, which result in the formation of  $\pi$ - or  $\sigma$ -complexes with various degrees of charge transfer. On the basis of the presented X-ray crystallographic evidence, we develop a donor–acceptor or charge-transfer concept that satisfactorily explains the structural details as well as the various facets of chemical reactivity of metal-coordinated arenes.

The donor–acceptor terminology for the description of organometallic coordination compounds is not new, since — in its conventional form — it considers a *formal* electron distribution merely based on Lewis acid–base interactions and electron count to determine how many electrons are donated by the arene ‘donor’ to provide a stable (18- or 16-electron, closed-shell) environment for the otherwise open-shell metal ‘acceptor’ [6]. In other words,  $\eta^1$ - through  $\eta^6$ -coordination [7] can be readily explained by this ‘donor–acceptor’ concept combined with the 18-electron rule. Although hapticity and electron count are extremely useful descriptors to classify organometallic complexes [7], they certainly do not satisfactorily explain the above mentioned structural features and the related chemical reactivity. To understand structural details such as the ring expansion of metal-coordinated arenes or the unusual bond strength in metal carbonyl complexes, additional electronic effects are commonly invoked — the most important being back-donation [6]. For example, in metal carbonyl complexes the vacant ( $\pi^*$ ) orbitals of the CO ligands are considered to interact with the (formally) occupied metal orbitals which leads to a redistribution of electrons and a strong metal–carbonyl bond. A closer look reveals that the back-donation concept is merely a *special* case of the *general* charge-transfer concept put forward in this review. In general, the description of organometallic substrates as ‘donor–acceptor’ complexes (with the ligand formally donating electrons to the metal center in accord with the 18-electron rule) does not provide any information on the *real* distribution of charges between metal and ligand. On the other hand, the charge-transfer concept considers the effective donor or acceptor strength<sup>1</sup> (see Section 2.1) of the ligand and the metal center and thus allows us to determine the actual location of charges and the degree of (metal-to-ligand or ligand-to-metal) charge transfer.<sup>2</sup>

We will first discuss a variety of structural (Section 2) and chemical (Section 3) effects in metal–arene complexes that arise from charge-transfer from and to the arene ligand. We will demonstrate with a few striking examples that the observed charge-transfer phenomena are independent of hapticity and/or electron count and, most importantly, have direct analogies in organic and inorganic donor–acceptor complexes. Detailed analyses of various  $\eta^1$ - and  $\eta^2$ -coordinated metal–arene complexes will then follow in Section 4 since structural and chemical effects of charge transfer are most pronounced in these low-hapticity complexes. To limit the scope of this review, we focus mostly on arene/transition-metal complexes, and donor–acceptor complexes with main-group metals are only discussed for comparison purposes.

<sup>1</sup> Donor and acceptor strength are generally gauged by the determination of ionization potentials and electron affinities (in the gas phase) or by oxidation and reduction potentials (in solution).

<sup>2</sup> According to Mulliken theory [8], charge transfer in a donor–acceptor complex is described by the wave function  $\Psi_{AD} = a\psi_0(A, D) + b\psi_1(A^-, D^+)$  with  $\psi_0$  and  $\psi_1$  being the ‘no-bond’ and the dative bonding functions, respectively. Accordingly, the degree of charge transfer is defined as the ratio  $b^2/a^2$  of the mixing coefficients [9,10].

## 2. Effects of charge transfer on the structure of metal–arene complexes

Several significant structural changes can be observed when aromatic hydrocarbons are coordinated to a metal center. Such effects include:

1. expansion of the aromatic ring;
2.  $\pi$ -bond localization in the arene ring;
3. distortion of planarity of the arene ring (either by folding or by deviation of the position of substituents out of the plane of the ring);
4. shortening of the arene–metal bond distance (from van der Waals contact to covalent ( $\sigma$ ) bonds).

Moreover, there are striking examples of secondary intermolecular interactions that are observed between metal–arene complexes and additional donor or acceptor molecules that are caused by a donor–acceptor *umpolung* of the arene ligand.

It needs to be emphasized that all the above listed structural features are not unique to arene–metal complexes, but they are also found (to various degrees) in other complexes of arenes with organic or inorganic donor–acceptor counterparts. In the following paragraphs, we will demonstrate this analogy between organic, inorganic, and organometallic electron donor–acceptor (EDA) complexes from which we conclude that all structural phenomena can be explained by a unifying concept of charge transfer which is generally applicable to all types of EDA complexes — from inorganic to organic to organometallic substrates, from  $\pi$ - to  $\sigma$ -bonding, and from  $\eta^1$ - to  $\eta^6$ -coordination.

### 2.1. Expansion of the arene ring

On the basis of molecular orbital theory, ring expansion of arenes in donor–acceptor complexes is expected in two very different cases: (a) when the arene acts as an electron donor and thus suffers from electron deficiency in its HOMO  $\pi$ -bonding orbitals; and (b) when the arene acts as an electron acceptor and thus experiences partial population of its LUMO  $\pi^*$ -antibonding orbitals. In more quantitative terms, the orbital population and the resulting bond order in benzene is described as follows: The ring of six carbon atoms in benzene is held together by six  $\sigma$ -bonds (involving two electrons each) and six  $\pi$ -electrons which occupy three delocalized  $\pi$ -bonding orbitals. Thus, the total count for bonding orbitals consists of 18 electrons, which are involved, in the six carbon–carbon bonds. Since a chemical bond of unit order requires two electrons, the average bond order in the aromatic ring is  $b_{av} = 1.5$ . Removal of an electron from a bonding orbital (to form the arene cation radical) or addition of an electron into an antibonding orbital (to form the arene anion radical) both lead to a decrease in the average bond order in the arene ring as the result of the loss (or annihilation) of one bonding electron, i.e.  $b_{av} = 17/(6 \times 2) = 1.42$ .

According to Pauling [11], there is a direct exponential relationship between bond order and bond length given by the general formula:

$$d_N = d_1 - k \log N \quad (1)$$

Table 1

Relationship between bond order and bond distance in the benzene ring<sup>a</sup>

| Bond order | Bond length (Å) | Bond order | Bond length (Å) |
|------------|-----------------|------------|-----------------|
| 1.0        | 1.486           | 1.5        | 1.398           |
| 1.1        | 1.465           | 1.6        | 1.384           |
| 1.2        | 1.446           | 1.7        | 1.371           |
| 1.3        | 1.429           | 1.8        | 1.358           |
| 1.4        | 1.413           | 1.9        | 1.347           |
|            |                 | 2.0        | 1.335           |

<sup>a</sup> Calculated according to Eq. (1) [11].

where  $d_N$  is the bond length for bond order  $N$ ,  $d_1$  is the bond length for unit bond order, and  $k$  is an empirical coefficient specific for a particular combination of atoms. Using Eq. (1) with  $k = 0.5$ ,  $d_1 = 1.49$  Å for a single bond between two (non-conjugated)  $sp^2$ -hybridized carbon atoms, and  $d_2 = 1.33$  Å for a non-conjugated double bond between two ( $sp^2$ -hybridized) carbon atoms [12], we can calculate the bond orders  $N$  for various distances  $d_N$  and vice versa (Table 1). For example, the average bond order of  $b_{av} = 1.5$  expected for the neutral benzene ring (vide supra) leads to a calculated bond length of  $d = 1.398$  Å, which is indeed the experimental value obtained from low-temperature (15 K) neutronographic measurements [13]. On the other hand, the average bond length in benzene cation radical with a bond order of  $b = 1.42$  is predicted to be  $d_{av} = 1.410$  Å, which differs from that in neutral benzene only by  $\Delta d_{av} \approx 0.01$  Å. Thus, in order to identify aromatic cation radicals from the average ring expansion of  $\Delta d_{av} \approx 0.01$  Å per C–C bond, the precision of the X-ray crystallographic data must be far better than  $\pm 0.01$  Å. Unfortunately, the vast majority of organometallic structures are carried out (at best) with a precision in the same range as the predicted bond elongations, and they are thus not suitable to reveal electron deficiencies or partial cation-radical character in arene ligands of organometallic EDA complexes.

Recent advances in the use of low-temperature X-ray diffractometers have improved the precision significantly (up to  $\pm 0.001$  Å) which makes it now possible to distinguish between neutral arenes and their cation radicals by their average C–C bond distance. For example, X-ray crystallographic data of hexamethylbenzene (HMB) at  $T = -150^\circ\text{C}$  obtained recently in our laboratory [14] reveal an average bond length of  $d_{av} = 1.411(1)$  Å between the six ring atoms.<sup>3</sup> Although the structure of  $\text{HMB}^{+\bullet}$  cation radical has not been determined up to now, there are several precise structures of EDA complexes of hexamethylbenzene with various organic and inorganic acceptors available, the precision of which allows us to determine the ring expansion in the complexed arene as compared to the structure of neat hexamethylbenzene crystals and thus to gauge the degree of charge transfer from

<sup>3</sup> Elongation of the average C–C bond length  $d_{av}$  in HMB by 0.013 Å as compared to unsubstituted benzene is apparently caused by steric repulsion and by a strong inductive effect of the methyl substituents.

HMB donor to the acceptor moiety. For example, EDA complexes of HMB with inorganic acceptors show substantial degrees of charge transfer as determined by IR and  $^{13}\text{C}$ -NMR spectroscopy [15], and accordingly, high-precision X-ray structures clearly reveal significant expansion of the arene ring. In particular, the average bond length ( $d_{\text{av}}$ ) in crystalline EDA complexes of HMB with nitrosyl hexafluoroantimonate ( $\text{NO}^+ \text{SbF}_6^-$ ) or nitrosyl hexafluorophosphate ( $\text{NO}^+ \text{PF}_6^-$ ) was determined to be  $d_{\text{av}} = 1.415(2)$  [16] and  $1.416(2)$  Å [17], respectively. A similar ring expansion with  $d_{\text{av}} = 1.417(2)$  Å was found for EDA complexes of hexamethylbenzene with  $\text{SbCl}_3$  [18]. According to Pauling equation (Eq. (1), [11]), such changes in the average bond length corresponds to the charge transfer of ca. 0.5 electrons from HMB to the inorganic acceptor.<sup>4</sup>

The degree of charge transfer in EDA complexes of various substituted benzenes with the same acceptor strongly depends on the donor strength of the arene as gauged by its ionization potential (Table 2).

This effect of the arene donicity has been demonstrated with arene–nitrosonium complexes [15], in which the degree of charge transfer from the arene donor to the  $\text{NO}^+$  acceptor was determined from the N–O stretch frequencies ( $\nu_{\text{NO}}$ ) in the IR spectra. With increasing donor strength of the arene, a shift of  $\nu_{\text{NO}}$  to lower frequencies is observed which correspond to lower bond orders and longer bond lengths in the NO moiety due to partial charge transfer. In fact, from the N–O stretch frequency in the HMB complex which is close to that of (neutral) nitric oxide, a degree of charge transfer of 97% is computed [15]. EDA complexes of

Table 2  
Ionization potentials (IP) of various substituted benzenes

| R-substituted benzene, R = | IP (eV) <sup>a</sup> |
|----------------------------|----------------------|
| H                          | 9.23                 |
| Chloro                     | 9.08                 |
| Bromo                      | 9.05                 |
| Methyl                     | 8.82                 |
| 1,2-Dimethyl               | 8.56                 |
| 1,4-Dimethyl               | 8.44                 |
| 1,2,4-Trimethyl            | 8.27                 |
| 1,3,5-Trimethyl            | 8.42                 |
| 1,2,4,5-Tetramethyl        | 8.05                 |
| Pentamethyl                | 7.92                 |
| Hexamethyl                 | 7.85                 |

<sup>a</sup> From Ref. [15].

<sup>4</sup> The average C–C bond length  $d_{\text{av}} = 1.416$  Å found in the EDA complexes of **HMB** with inorganic acceptors corresponds to an average bond order  $b_{\text{av}} = 1.380$  whereas  $d_{\text{av}} = 1.411$  Å in neat HMB crystals indicates a formal bond order of  $b_{\text{av}} = 1.413$ . The difference of 0.033 in the bond order of each carbon–carbon bond results in a total bond-order difference of  $\Delta b_{\text{av}} = 0.033 \times 6 = 0.198$  for the entire benzene ring, which corresponds to a loss of  $(0.198 \times 2) \approx 0.4$  electrons from the bonding orbitals of the arene molecule.

arene donors with organic acceptors generally show much lower degrees of charge transfer, and therefore ring expansion can hardly be detected. For example, the EDA complex of hexamethylbenzene with chloranil exhibits an unchanged (within the precision of the measurement) arene moiety with  $d_{\text{av}} = 1.409(2)$  Å [19]. We estimate the degree of charge transfer in this EDA complex to be too small (less than 10%) to be detected by X-ray crystallography even at a precision of  $\pm 0.002$  Å.

In contrast, many organometallic complexes with arene ligands show degrees of ring expansion that widely exceed those reported above for organic and inorganic acceptors. For example, an average C–C bond length of  $d_{\text{av}} = 1.422$  Å was obtained for the tripod complexes  $[(\text{HMB})\text{TiCl}_3]\text{AlCl}_4$  [20] and  $[(\text{HMB})\text{Mn}(\text{CO})_2\text{Cl}]$  [21]. Similarly,  $(\text{HMB})\text{Cr}(\text{CO})_3$  ( $d_{\text{av}} = 1.423$  Å) [22] and  $[(\text{HMB})_2\text{Fe}][\text{C}(\text{CN})_3]_2$  ( $d_{\text{av}} = 1.424$  Å) [23] show significant ring expansion in the HMB ligands. Extreme bond elongation ( $d_{\text{av}} = 1.429$  and  $1.430$  Å, in two symmetrically independent molecules) were found in the ruthenium complex  $(\text{HMB})\text{RuCl}_2(\text{py})$  [24]. According to the Pauling equation (see Eq. (1), [11]), such long bond distances reveal a charge transfer of ca. 1.4 electrons between the HMB ligand and the metal center! Such significant re-distribution of charges leading to a substantial electron deficiency in the arene ligand is expected to have striking consequences for the reactivity of metal-coordinated arenes up to the point of complete electrophilic–nucleophilic *umpolung* of its substitution behavior (vide infra).

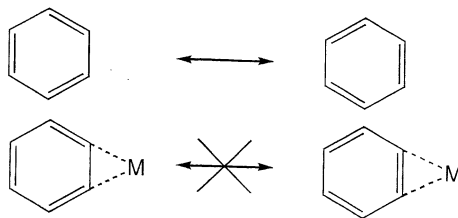
## 2.2. $\pi$ -Bond localization in the arene ring

The localization of  $\pi$ -bonds (also termed ‘double-bond fixation’) is an important structural feature frequently observed upon coordination of an arene ligand to a metal center. To understand this effect, the formation of covalent ( $\sigma$ ) bonds between the metal and particular carbon atoms of the arene ring is commonly invoked. However, this valence-bond approach cannot explain all unusual bond distances and is not generally applicable to analogous findings with organic or inorganic complexes. We prefer an analysis based on the charge-transfer concept, which not only allows a comparative treatment of all types of donor–acceptor complexes, but also predicts a close relationship between the degree of bond localization and the donor–acceptor strength of the complex partners. To demonstrate this point, we will examine several examples with  $\eta^2$  complexes, but emphasize that bond localization is most pronounced, but by no means unique for this coordination mode.

During  $\eta^2$ -coordination with a metal center, the two mesomeric structures of the benzene ligand are expected — at first glance — to lose their equivalent state which leads to bond fixation (see Scheme 1).

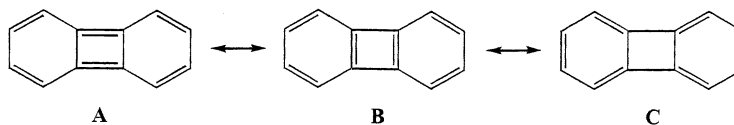
However, the various examples discussed in this section will show that this simple model only applies in cases of significant degrees of charge transfer between the benzene ligand and the metal center. In other words,  $\eta^2$ -coordination alone does not cause the degradation of the delocalized electronic configuration of the aromatic ligand. This is best illustrated with two complexes of arenes with carbon

tetrabromide, an organic acceptor, and silver(I), an inorganic acceptor. Both the [durene,  $\text{CBr}_4$ ] complex [25] and [benzene,  $\text{Ag}^+\text{ClO}_4^-$ ] [26] are considered as very weak EDA complexes which exhibit very low degrees of charge transfer. Thus, it is not surprising that changes in the C–C bond lengths in the complexed arenes do not exceed 0.01 Å as compared to those extant in the neutral molecules.



Scheme 1.

On the other hand, if the aromatic resonance is already distorted in the neutral (uncomplexed) arene as it is the case for various condensed aromatics due to steric and electronic effects, significant changes in bond localization may be achieved even by relatively weak charge-transfer interactions. For example, biphenylene in its neutral state exhibits three non-equivalent resonance forms with the highest contribution stemming from structure C (see Scheme 2).

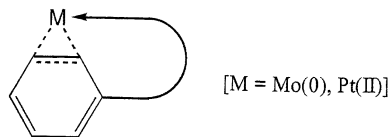


Scheme 2.

In contrast, X-ray structural data of the octamethylbiphenylene cation radical salts with tetracyanoethylene (TCNE) or tetracyanoquinodimethane (TCNQ) anion radicals as counter ions clearly exhibit structure A as predominant. Interestingly, the X-ray structure of (biphenylene) $\text{Cr}(\text{CO})_3$  shows a bond alternation in the biphenylene ligand very similar to that observed in its cation-radical structure [27]. We conclude that this chromium complex exhibits a very high degree of charge transfer (ca. 1 electron) between the biphenylene ligand and the metal center.

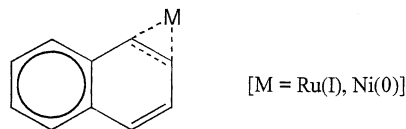
This conclusion is in line with our general finding that organometallic substrates exhibit a large range of degrees of charge-transfer, which are readily revealed by X-ray structural investigations. Other examples include  $\eta^2$  complexes of molybdenum(II) and platinum(II) with substituted benzene ligands. Bond contraction of the two non-coordinated  $\pi$  bonds of up to 1.37 and 1.35 Å have been found for Mo(0) [28] and Pt(II) [29] complexes, respectively, which corresponds to bond orders of 1.7 and 1.9, respectively (see Scheme 3).





Scheme 3.

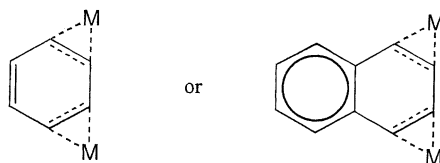
Stronger arene donor ligands such as naphthalene or anthracene show even more pronounced double-bond fixation as established for ruthenium(I) [30] and nickel(0) [31] complexes (see Scheme 4).



Scheme 4.

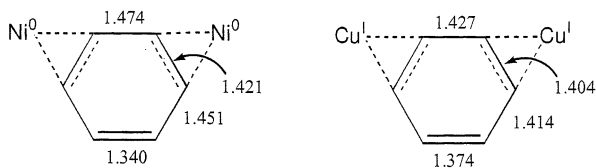
Here, the non-coordinated C( $\alpha$ )–C( $\beta$ ) bond clearly approaches the standard value of 1.34 Å for a normal carbon–carbon double bond.

The localized double bond is not only identified by its short distance, but also by its capability to coordinate to other metal centers in the same way as olefinic ligands. As a result,  $\mu$ - $\eta^2$  complexes are formed with the general structures shown in Scheme 5.



Scheme 5.

Two examples need to be mentioned which convincingly demonstrate the effects of different degrees of charge transfer on the bond-length distribution within the benzene ring. The two *isoelectronic* complexes of benzene with nickel(0) [32] and copper(I) [33] with the same hapticities and double-coordinated structures exhibit very different bond-length distributions (see Scheme 6).



Scheme 6.

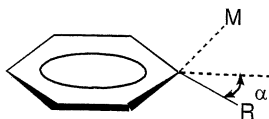
Thus, merely the difference in the acceptor strength of nickel(0) as compared to copper(I) causes a much stronger  $\pi$ -electron redistribution in the nickel complex with bond-length changes of more than 0.04 Å, which correspond to a charge relocation of ca. 0.5 electrons within the aromatic ring.

In summary,  $\pi$ -bond localization in metal-coordinated arene ligands as revealed by X-ray crystallography represents a striking piece of evidence for charge-transfer interactions between arene donor and metal acceptor in organometallic complexes. Such  $\pi$ -electron re-distribution within the aromatic ring is expected to ultimately lead to a complete change in the chemical reactivity of the arene ligand from aromatic to olefinic reactivity.

### 2.3. Loss of planarity of the arene ring

The planar structure of the six-carbon ring is a general characteristic of undistorted aromatic substrates. In other words, the planarity of the  $\pi$ -conjugated system is a prerequisite for its aromatic character and any loss of it either by deviations of the positions of substituents out of the plane or by actual folding of the six-carbon ring diminishes or even completely annihilates its aromaticity. In fact, coordination of planar arenes to metal centers may cause a loss of planarity of the six-carbon ring, and we will show in this section that such distortion of the planarity of arene ligands in organometallic complexes can be induced by charge-transfer interactions between the arene and the metal center. However, such effects are only observed in those cases involving rather high degrees of charge transfer.

For example, in  $\eta^1$  complexes we frequently observe a deviation of the substituent attached to the coordinated (*ipso*) carbon atom out of the aromatic plane and away from the coordinating metal center (M) (see Scheme 7).

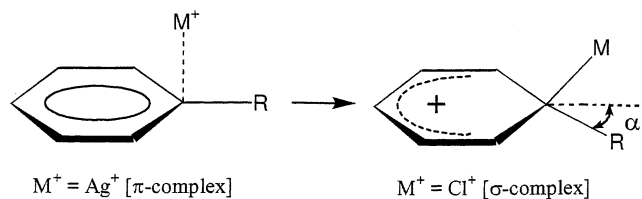


Scheme 7.

Such deviations are well documented for  $\eta^1$  complexes of chromium(II), cobalt(II), nickel(II), and platinum(II) with substituted benzenes, and the deviation angle  $\alpha$  varies between  $2^\circ$  in  $[\text{Cr}(\text{NMesBMes}_2)_2]$  [34] and  $22^\circ$  in  $[\text{Pt}(o\text{-Tol})(\text{MeC}_6\text{H}_3(\text{CH}_2\text{NMe}_2)_2\text{-}o,o')\text{I}]$  complexes [35].

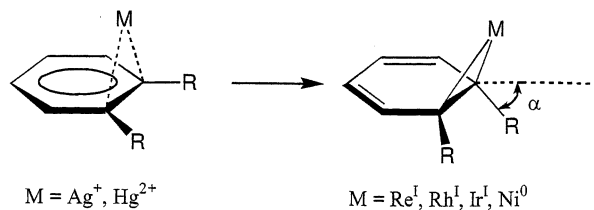
Such bending of the *ipso* substituent out of the aromatic plane due to complex formation is not only observed with organometallic complexes, but has numerous analogues in other arene complexes with organic or inorganic counterparts. Independent of the nature of the complex partner, there is a clear trend between the bending angle ( $\alpha$ ) and the degree of charge transfer from the arene donor to the coordinated acceptor. For example, in weak ( $\pi$ )-complexes of silver(I) with arenes [36,37] no deviation of the *ipso* substituent R out of the plane is observed ( $\alpha \approx 0$ ). Complexes of copper(I) [36], triethylsilyl ( $\text{Et}_3\text{Si}^+$ ) [38], and triarylaluminum [39] with arenes show small but significant deviation angles of  $\alpha = 7, 8$ , and  $9^\circ$ , respectively, which are symptomatic of an increasing  $\sigma$ -character in the coordination of the metals as opposed to the pure  $\pi$  character of the  $\text{Ag}^+$  coordination (vide supra). The change from  $\pi$ - to  $\sigma$ -character implies an increasing degree of charge

transfer from the arene donor to the coordinated acceptor, which leads in its extreme form to the classic  $\sigma$ -complexes in which the positive charge of the inorganic component is completely transferred to the arene. For example, bending angles of  $\alpha = 42$  and  $55^\circ$  have been determined by X-ray crystallographic studies of crystalline  $\sigma$ -complexes of bromonium ( $\text{Br}^+$ , with  $\text{SbF}_6^-$  counter anion) [40] and chloronium ( $\text{Cl}^+$ , with  $\text{SbCl}_6^-$  counter anion) [41] with hexamethylbenzene (Scheme 8).



Scheme 8.

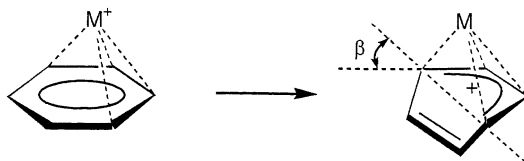
In  $\eta^2$  complexes, similar trends are observed on going from weak  $\pi$ -complexes with low degree of charge transfer to  $\sigma$ -complexes with high charge-transfer character. For example, silver(I) [26] and mercury(II) [42] complexes with arenes exhibit bending angles of  $\alpha \approx 5^\circ$ , which are symptomatic of high  $\pi$ -character of the complex or low degree of charge transfer. In contrast,  $\eta^2$  complexes of late transition metals such as rhenium, rhodium, iridium, nickel, etc. with arenes exhibit bending angles ( $\alpha$ ) of up to  $45^\circ$  [43] (see Scheme 9).



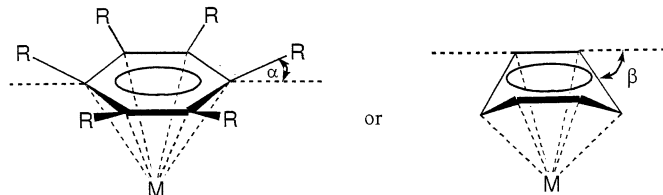
Scheme 9.

In its extreme case, charge-transfer interactions in arene–metal complexes do not only affect the planar position of arene substituents (R), but also the planarity of the arene ring itself. Various degrees of ring folding are observed in  $\eta^4$ -coordinated complexes of benzene with metal centers ranging from folding angles of  $\beta = 0^\circ$  in alkaline metal salts,  $\beta \approx 15^\circ$  in lanthanide complexes [44], and  $\beta \approx 30\text{--}35^\circ$  in early transition-metal complexes (e.g. titanium, zirconium [45]) to the highest degree of folding in iron and ruthenium complexes ( $\beta \approx 40^\circ$ ) [46]. Interestingly, arene complexes with late transition metals such as cobalt ( $\beta \approx 35^\circ$ ) [47] and nickel ( $\beta \approx 20\text{--}25^\circ$ ) [48] again show lower folding angles (Scheme 10).

Both types of distortion of the planarity of the arene ring, viz. bending of *ipso*-substituents and folding of the carbon six ring are observed in  $\eta^6$ -coordinated metal–arene complexes (see Scheme 11).



Scheme 10.



Scheme 11.

For example, whereas the six-carbon ring remains more or less planar in most d-metal complexes of benzene and distortion of the aromaticity is only manifested in various degrees of bending of the arene substituents out of the ring plane, significant folding of the arene ring to a boat-type shape is observed in complexes of benzene with tantalum. Interestingly, the degree of folding depends on the oxidation state of the metal, i.e.  $\beta \approx 20^\circ$  for  $\text{Ta}^{2+}$  [49] and  $25^\circ$  for  $\text{Ta}^{3+}$  [50] complexes. Obviously, the better electron acceptor, tantalum(III), causes a stronger folding due to a higher degree of charge transfer from the benzene ring to the tantalum center and consequently a higher degree of  $\sigma$ -character in the arene/metal bonds.

#### 2.4. The metal–arene bonding distance

The distance between two atoms that either reside within the same molecule or belong to two separate molecular entities is the most commonly used measure to gauge the strength of the intramolecular or intermolecular chemical bond between the two nuclei. Charge-transfer interactions, which strengthen the intermolecular bond between a donor and an acceptor molecule, are expected to cause significant bond shortening relative to the distance of purely van der Waals contact of the two atoms. For example, the interplanar distance of  $d = 3.42 \text{ \AA}$  between hexamethylbenzene and chloranil in their mixed-stack charge-transfer crystals [19] is shortened by  $0.2 \text{ \AA}$  as compared to the intermolecular distance of  $d = 3.62 \text{ \AA}$  in neat hexamethylbenzene crystals [14]. Even stronger changes in intermolecular distances due to charge-transfer interactions are found in crystalline charge-transfer complexes between organic donors and inorganic acceptors. For example, the distance between nitrosonium ion and the aromatic ring in crystalline arene/ $\text{NO}^+$  complexes varies from  $d = 2.50 \text{ \AA}$  in complexes with the weak donors benzene ( $\text{NO}^+ \cdot \text{SbCl}_6^-$

·3Bz [51]) and toluene ( $\text{NO}^+ \cdot \text{AlCl}_4^- \cdot 3\text{MePh}$  [52]) to  $d = 2.09 \text{ \AA}$  for the EDA complex with the much stronger donor hexamethylbenzene [16]. Similarly, the distance between gallium and the aromatic ring in arene- $\text{Ga}^+$  complexes varies between  $d = 2.76 \text{ \AA}$  for benzene [53] and  $d = 2.42 \text{ \AA}$  in the hexamethylbenzene complex [54].

Analogous trends in the distance variation with the donor–acceptor properties of the complex partners are found in  $\pi$ -complexes of d-metals with aromatic ligands. For example, the niobium(0)/arene distance is decreased by  $0.010 \text{ \AA}$  when the donor strength of the arene ligand is increased from the *bis*(toluene) complex ( $d = 1.860 \text{ \AA}$ ) [55] to the *bis*(mesitylene) complex ( $d = 1.850 \text{ \AA}$ ) [56]. A comparison of arene complexes with metals of different acceptor strength confirms the effect of charge transfer on the intermolecular distance. For example, the distance between arene ligand and chromium center is reduced by  $0.015 \text{ \AA}$  in *bis*(benzene)chromium(I) bromide ( $d = 1.597 \text{ \AA}$ ) [57] as compared to the corresponding *bis*(benzene)chromium(0) complex ( $d = 1.612 \text{ \AA}$ ) [58].

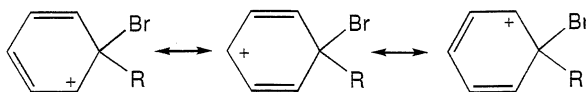
Frequently, organic ligands in transition metal complexes penetrate the coordination sphere of the d-metal to such an extent that ligand-to-ligand distances of much less than the sum of the van der Waals radii are observed. In these cases, effects of coulombic forces or steric repulsion become very important and often control the metal–arene distance. For example, charge transfer from two equal or similar donor ligands to a metal center may become so strong that the resulting positive charges on both ligands lead to mutual (Coulombic) repulsion. Such effects may even overcompensate the distance-shortening effects of the charge transfer and eventually cause an *increase* in the arene–metal distance with increasing donicity of the arene ligand. Accordingly, the  $\text{Ru}^{2+}$ –arene distance in the *bis*(benzene) complex ( $d = 1.713 \text{ \AA}$ ) [59] is shorter than that in the corresponding *bis*(mesitylene) complex ( $d = 1.726 \text{ \AA}$ ) [60] probably due to increased Coulombic repulsion and/or steric hindrance between the two mesitylene ligands bearing partial positive charges.

Metal–arene distances in organometallic donor–acceptor complexes do not reveal the direction of charge transfer, viz. from the ligand to the metal or vice versa. This is illustrated with two isoelectronic and isosteric  $\text{CpIr}(\text{arene}) \eta^4$  complexes. Both the hexafluorobenzene complex ( $d = 2.10 \text{ \AA}$ ) [61] and the hexamethylbenzene complex ( $d = 2.12 \text{ \AA}$ ) [62] exhibit very similar  $\text{Ir}^+$ –arene distances despite the substantial difference in the donor–acceptor properties of the two arene ligands. By contrast, the  $\text{Ir}^+$ –Cp distance decreases significantly ( $\Delta d = 0.05 \text{ \AA}$ ) when the hexamethylbenzene ligand is replaced by hexafluorobenzene. Obviously, the (hexafluorobenzene) $\text{Ir}^+$  moiety is a stronger acceptor than the (hexamethylbenzene) $\text{Ir}^+$  moiety and thus exhibits a stronger charge-transfer bonding to the cyclopentadienyl donor ligand. Most remarkably, the arene– $\text{Ir}^+$  distance in a similar (tripphosphine)iridium complex with (unsubstituted) benzene [63] is ca.  $0.1 \text{ \AA}$  longer than that in the hexafluorobenzene or hexamethylbenzene complexes mentioned above. Apparently, in the triphosphine(benzene) $\text{Ir}$  complex the donor–acceptor properties of the triphosphine iridium moiety and the benzene ligand are more or less equal, and no significant charge-transfer bonding between iridium and benzene ligand is observed.

## 2.5. Change of donor–acceptor properties of metal-coordinated arene ligands

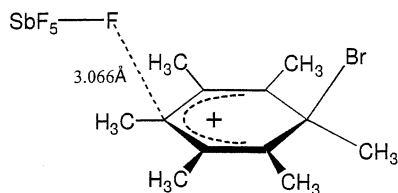
Charge-transfer interactions between arene ligand and metal center in an organometallic complex result in significant changes of the donor or acceptor strength of the ligand due to the build-up of electron deficiency or electron excess in the aromatic ring. For example, complete charge transfer from the arene donor to the metal center effects the generation of a positive charge on the arene ligand which enables the arene to bond with a negatively charged species. In more general terms, the charge-transfer interaction of the arene ligand with the metal center converts the electron-rich donor into an electron-poor acceptor, or — in other words — the coordinated arene becomes a target of nucleophilic attack. The *chemical* consequences of such an electrophilic/nucleophilic *umpolung* will be discussed in detail in a later section. At this stage, we will analyze the structural aspects of new intermolecular interactions between coordinated arenes and additional donors or acceptors to reveal external charge-transfer interactions of the metal–arene complex.

Electrophilic–nucleophilic *umpolung* is not restricted to arene ligands coordinated to metal centers, but it is commonly observed in crystalline complexes of aromatic donors with organic or inorganic acceptors. For example, the complete charge transfer from hexamethylbenzene to bromonium upon the formation of the bromoarene  $\sigma$ -complex leads to a delocalized positive charge on the arene six-ring (see Scheme 12).



Scheme 12.

As a result, such positively charged  $\sigma$ -complexes readily react with a variety of nucleophiles and can be stabilized (and crystallized) only in the presence of very weak nucleophiles such as hexachloroantimonate, hexafluorophosphate, or similar counter anions [64]. However, X-ray crystallographic studies clearly reveal that even such weak nucleophiles exhibit strong interactions with the positively charged arenium as evidenced by unusually short intermolecular distances. For example, in crystalline complexes of bromohexamethylbenzenium hexafluoroantimonate [40], there is a close contact between fluorine and the carbon atom in *para*-position to the bromine atom with a shortened F–C distance of 3.066 Å as compared to the sum of the van der Waals radii of  $d = r_F + r_C = 3.17$  Å [65] (see Scheme 13).



Scheme 13.

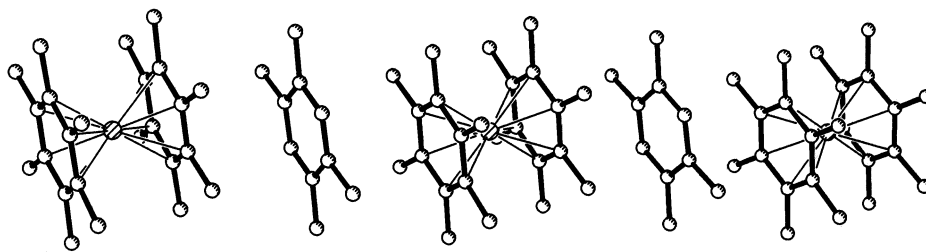


Fig. 1. Stacking of the crystalline EDA complex of *bis*(hexamethylbenzene) iron(II) with durene (donor–acceptor distance  $d = 3.65$  Å).

Evidently, in these crystals the hexafluoroantimonate or — to be precise — one of its fluorine atoms acts as an electron donor that bonds to hexamethylbenzene which is positively charged due to complete charge-transfer to the bromonium and thus acts as the acceptor.

Similar structural effects of donor–acceptor *umpolung* of arene ligands are known with organometallic complexes. Again, we choose hexamethylbenzene as example, which as a strong electron donor forms numerous EDA complexes with organic, inorganic and organometallic acceptors. However, if hexamethylbenzene is coordinated to a strong electron acceptor, its donor strength is completely annihilated and it is now capable of forming EDA complexes with other (even weaker) donors. For example, the hexafluorophosphate salt of *bis*(hexamethylbenzene)iron(II) forms EDA complexes with durene in solution as established by the observation of charge-transfer absorption bands [66]. The crystal structure of the EDA complexes shows alternate stacks of durene with *bis*(arene)iron(II) in which the interplanar distance between durene and hexamethylbenzene amounts to  $d = 3.65$  Å (see Fig. 1).

This close distance and the absorption spectrum of the complex point to substantial charge-transfer interactions between durene as the donor and hexamethylbenzene which acts as the acceptor due to its high electron deficiency caused by the coordination to the electron-poor iron(II) center.

### 3. Charge-transfer activation of metal-coordinated arene ligands

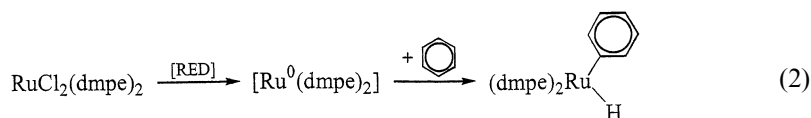
The structural changes in arenes upon coordination with a metal center as illustrated in the previous section, would be of little interest if there were not closely related to the reactivity of organometallic complexes. In fact, arene–metal complexes are crucial intermediates in homogeneous metal catalysis [1–5], which means that the coordination of an aromatic substrate to a metal center changes its chemical properties to such an extent that reactions readily occur which are not possible with the free (uncomplexed) arene. Numerous new reactions of arenes have

been discovered over the years exploiting the catalytic effects of metals that bond to the arenes to form (stable or transient) organometallic complexes [1–5]. Interestingly, the catalytic effect of metals on arene reactivity is principally different from that of other catalysts, which generally enhance the reactivity of the agents attacking the arene substrate. For example,  $\text{AlCl}_3$  or silver(I) salts catalyze aromatic halogenation reactions by promoting the heterolytic cleavage of the dihalogen bond. In contrast, metal catalysts enhance the reactivity of the arene substrates so that even weak reagents can be effectively used for the chemical transformation.

In the previous section, we have shown that various changes in the arene structure upon metal coordination can be understood on the basis of the charge-transfer concept. Charge-transfer interactions cause a series of electronic and structural changes (such as  $\pi$ -bond localization, electron deficiency, ring folding, etc. *vide supra*) which ultimately lead to the loss of aromaticity in the arene ligand. Thus, the conclusion is obvious that the very same charge-transfer interactions that cause the structural changes are also responsible for the changes in reactivity of metal-coordinated arenes. In fact, changes in structure and reactivity are closely related since both are controlled by the location and density of valence electrons within the organometallic complex. We will demonstrate in this section that metal-coordinated arene ligands exhibit a different reactivity as compared to the free arenes due to charge-transfer interactions with the metal center. For this purpose, we do not intend to cover a wide variety of organometallic reactions, but we will restrict our attention to two more general effects observed in metal–arene complexes, viz. (i) carbon–hydrogen bond activation and (ii) nucleophilic–electrophilic *umpolung*.

### 3.1. Carbon–hydrogen bond activation

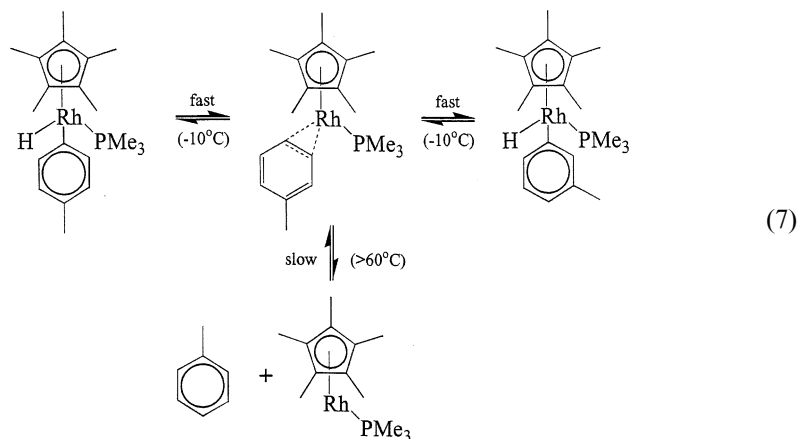
Carbon–hydrogen bond activation of arenes by transition-metal complexes in solution is known since the 1970s — one of the earliest examples being the oxidative addition of benzene, naphthalene, and other aromatic hydrocarbons to the reduction product of  $\text{RuCl}_2(\text{dmpe})_2$  [ $\text{dmpe} = (\text{CH}_3)_2\text{P}-\text{CH}_2\text{CH}_2-\text{P}(\text{CH}_3)_2$ ] to yield arylruthenium hydrides [67,68]:



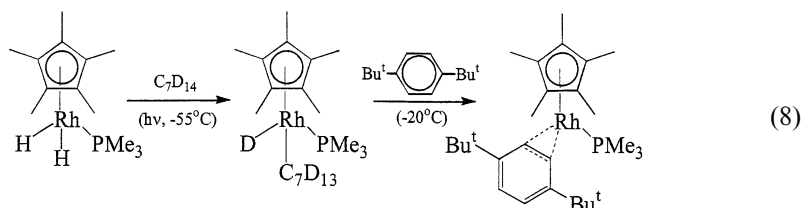
Such C–H bond activations in oxidative additions to metal centers have been utilized for a variety of chemical transformations of arenes including H/D exchange and substitution reactions. For example, H/D exchange in arenes is promoted by various transition metal complexes including high-valent species such as  $\text{Ta(V)}\text{H}_3(\text{C}_2\text{H}_5)_2$ , low-valent species like  $\text{Ru}^0(\text{dmpe})_2$  (see Eq. (2)), or  $\text{Pd(II)}$  and  $\text{Pt(II)}$  complexes [69]. Substitution reactions include silylations [70], carboxylations [71], phenylimine formation [72], etc. which may occur by direct coupling of the



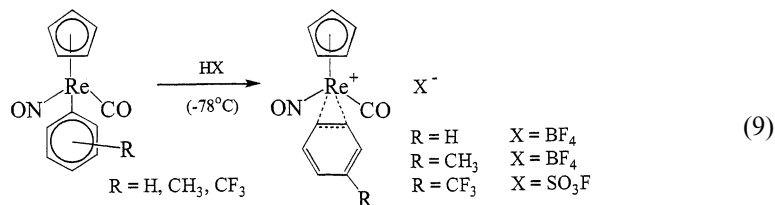




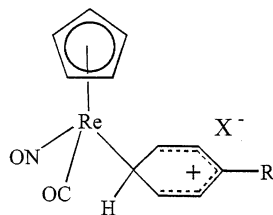
In fact, a stable  $\pi$  complex of *para*-di-*tert*-butylbenzene with the coordinatively unsaturated  $\text{Cp}^*\text{Rh}(\text{PMe}_3)$  can be generated photolytically from  $\text{Cp}^*\text{Rh}(\text{PMe}_3)\text{H}_2$  in perdeuterated methylcyclohexane in the presence of di-*tert*-butylbenzene at low temperature [75], and the  $\eta^2$ -coordination has been established by  $^1\text{H}$ -NMR spectroscopy (see Eq. (8)).



Many  $\eta^2$  complexes of arenes with other metal centers including iridium [43], rhenium [76], mercury [42], etc. have been reported during the last three decades. Interestingly, rhenium  $\eta^2$  complexes with benzene, toluene, and trifluoromethylbenzene have been prepared from the corresponding aryl rhenium complexes by protonation at low temperature [76] (see Eq. (9)).

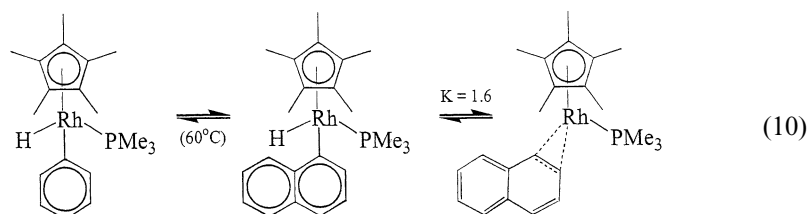


The  $^1\text{H}$ -NMR spectra of these complexes with five non-equivalent protons in the aromatic region has been explained by a migration of the rhenium group from one  $\eta^2$  position to another via the formation of an intermediate  $\eta^1$ -arenium complex of the following general structure [76] (see Scheme 14).



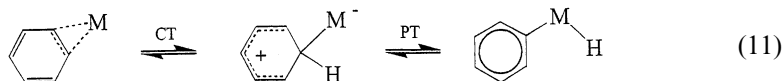
Scheme 14.

The stability of such  $\eta^2$  complexes strongly depends on the arene ligand and the metal center. For example, the  $\eta^2$  complex of naphthalene with rhodium exists in equilibrium with the naphthylhydrido complex at room temperature as detected by  $^1\text{H}$ -NMR spectroscopy [77] (see Eq. (10)).

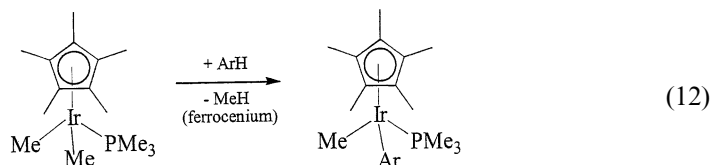


Similarly,  $\eta^2$  complexes with substituted naphthalenes, anthracene, phenanthrene, pyrene, fluoranthene, and triphenylene are stable at room temperature and have been identified by X-ray crystallography [77]. In all cases, the reversible interconversion of the  $\eta^2$  complex and the corresponding ( $\eta^1$ ) arylhydrido metal complex can be tuned by a variation of arene, metal center, and the other metal ligands [76].

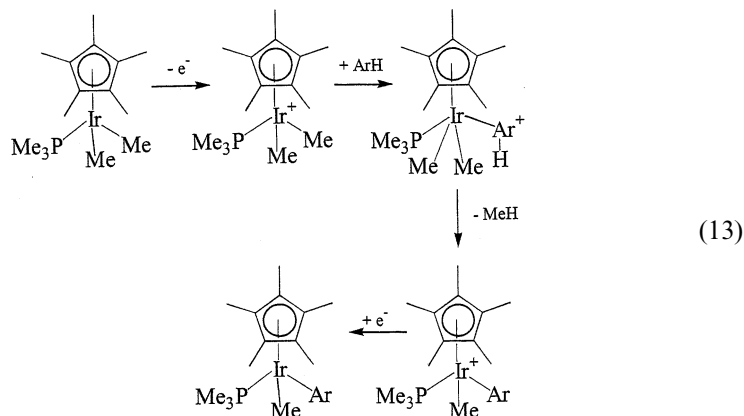
Such observations suggest that the pre-equilibrium complex formation between arenes and metal centers is a prerequisite for carbon–hydrogen bond activation. However, there is still a lack in understanding the mechanism of the interconversion between  $\eta^2$  complex and arylhydrido complex which formally represents a hydrogen-atom transfer between two tautomeric structures. To gain insight into the mechanisms of such tautomerisms, we now return to the charge-transfer character of metal–arene bonds which has been established for various organometallic complexes by a careful examination of their crystal structures (see Sections 2 and 4). The observation of charge transfer from the arene ligand to the metal does not only explain the structural features of metal–arene complexes, but also offers a simple explanation for a facile carbon–hydrogen bond activation. Thus, the net hydrogen-atom transfer from the arene to the metal can be conceived in two steps: First, charge transfer (CT) from the  $\pi$ -ligated arene to the metal center results in the formation of a  $\sigma$ -complex with delocalized positive charge on the arene ring, which then readily transfers a proton (PT) to the electron-rich metal center (see Eq. (11)).



In this context, a recent study on electron-transfer catalysis of carbon–hydrogen bond activation needs to be mentioned. C–H bond activation in various substituted arenes by  $\text{Cp}^*\text{Ir}(\text{Me})_2(\text{PMe}_3)$ , which leads to the corresponding monomethylaryl iridium complexes, is dramatically accelerated in the presence of catalytic amounts of one-electron oxidants such as ferrocenium [78] (see Eq. (12)).

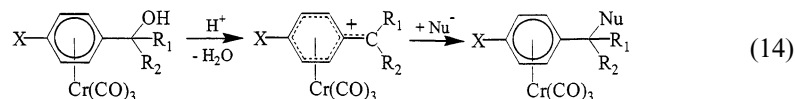


Obviously, the oxidized (17-electron) iridium complex readily activates even electron-poor arenes such as chloro-, nitro- and trifluoromethylbenzene. The electron-transfer chain mechanism formulated for this arene/methane ligand exchange [78] is not surprising in view of the above delineated charge-transfer mechanism for carbon–hydrogen bond activation. In the first step the arene substrate binds to the oxidized iridium center as a  $\pi$  ( $\eta^2$ ) complex. Owing to the strong acceptor strength of the electron-poor (17-electron) iridium group, complete charge transfer occurs from the arene to the metal, which results in the formation of a  $\sigma$ -arenium complex. This intermediate can readily transfer a proton to the methyl ligand to yield free methane and the oxidized methylaryl iridium complex, which is finally reduced by the original dimethyliridium complex to complete the ET chain process (see Eq. (13)).

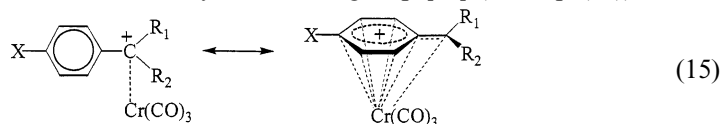


It is well established that electron-withdrawing transition metals coordinated to an arene not only activate aromatic carbon atoms (as described above) but also benzylic positions [79]. This finding has been exploited for synthetic purposes with a variety of  $\text{Cr}(\text{CO})_3$ ,  $\text{FeCp}^+$ , and  $\text{Mn}(\text{CO})_3^+$  complexes containing arene ligands. For example, depending on the substrates and the reaction conditions, benzylic carbon atoms of  $\text{Cr}(\text{CO})_3$ -coordinated arenes may be targets for nucleophilic or

electrophilic attack [79]. In the former case, a carbocation is generated under acidic conditions, which then reacts with the nucleophile (see Eq. (14)).

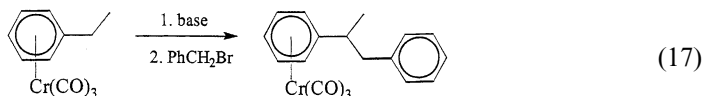
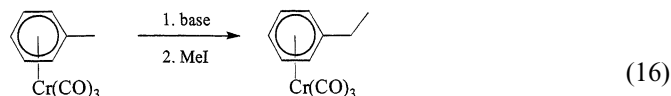


The coordination of the carbocation to the  $\text{Cr(CO)}_3$  center results in a substantial stabilization of this critical intermediate which is commonly explained either by interactions of filled d-orbitals of chromium with the empty p-orbital of the benzylic carbon or — more likely — by  $(\eta^7)$  coordination of the entire benzylic moiety (with a delocalized positive charge and partial double-bond character of the exocyclic C–C bond) to the tricarbonylchromium group [79] (see Eq. (15)).



In fact, both representations are based on the prediction that the  $\text{Cr(CO)}_3$  group acts as an electron donor, which interacts with the benzylic carbocation as the acceptor.

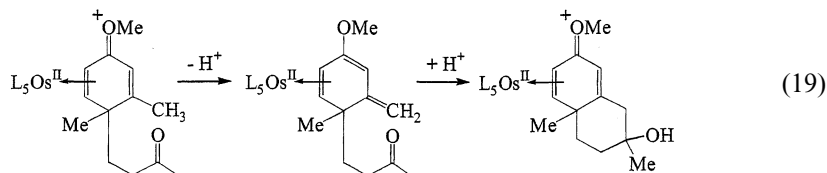
On the other hand, chromiumtricarbonyl is frequently considered as electron acceptor capable of stabilizing benzylic carbanions [79]. This conclusion is based on the fact that benzylic hydrogen atoms in  $(\text{arene})\text{Cr(CO)}_3$  are more acidic than in the corresponding free arenes [80–82]. For example, (toluene) $\text{Cr(CO)}_3$  can be deprotonated with bases such as alkoxides, potassium hydride, or LDA [83,84]. The resulting benzylic carbanion can then be trapped by various electrophiles (see Eqs. (16) and (17)).



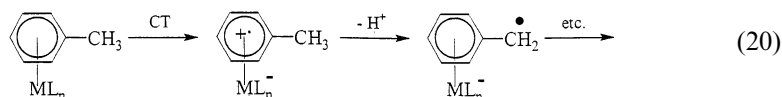
The facile deprotonation of benzylic positions is commonly explained by the stabilizing effect of the delocalization of the negative charge over the chromium moiety [79]. In other words, chromium acts now as electron acceptor, and complete charge transfer to the metal center would generate an exocyclic double bond and an  $\eta^5$ -coordinated negatively charged chromium center (see Eq. (18)).



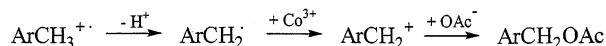
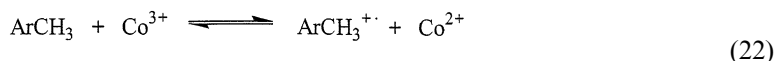
Enhanced deprotonation of benzylic carbon atoms is not restricted to (arene)Cr(CO)<sub>3</sub> complexes, but has also been found in  $\eta^6$ -coordinated Mn(CO)<sub>3</sub><sup>+</sup> [85] and FeCp<sup>+</sup> [4,86–88] complexes as well as in  $\eta^2$ -coordinated Os(II) complexes [89]. For example, deprotonation of the benzylic carbon of 3,4-dimethylanisol  $\eta^2$ -ligated to penta-amino-osmium(II) is a crucial step in the synthesis of functionalized decalins [89] (see Eq. (19)).



The stabilization of both benzylic carbocations and carbanions by donor–acceptor coordination to metal centers can be viewed as special cases of the more general charge-transfer concept promoted in this review. Particularly in the latter case, where metal-coordination of arenes leads to enhanced benzylic carbon–hydrogen bond activation, strong charge-transfer interactions between arene donor and metal acceptor prior to deprotonation are obviously responsible for the thermodynamic and kinetic acidity [85] of the metal-ligated arene. Based on the enhanced acidity of benzylic carbons in aromatic cation radicals [90,91], a charge-transfer scheme may be formulated which considers — in its extreme — a complete electron transfer from arene to the metal acceptor resulting in the formation of a cation-radical-type ligand which is readily deprotonated in benzylic positions (see Eq. (20)).



This reaction scheme is certainly applicable to C–H bond activation by *strong* electron acceptors. For example, the formation of benzyl acetate from toluene using Co(III) acetate as the oxidant has been shown to occur via the intermediate formation of toluene cation radical [92] (see Eqs. (21) and (22)).

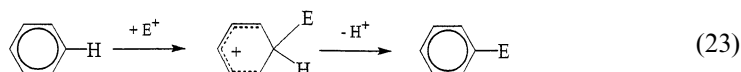


The electron-transfer mechanism is proposed based on the high value of  $\rho = -2.4$  obtained from the Hammett plots as well as the observation of benzyl chloride and chlorotoluene as the main products when the oxidation of toluene by Co(III) is carried out in the presence of high concentrations of lithium chloride [92]. Similarly, activation of benzylic carbon–hydrogen bonds by other strong oxidants such as manganese(III) or lead tetra-acetate has been suggested to occur via initial electron transfer especially in the case of aromatic substrates with low ionization potentials [93]. However, there are no reports of complex formation between the metal and the

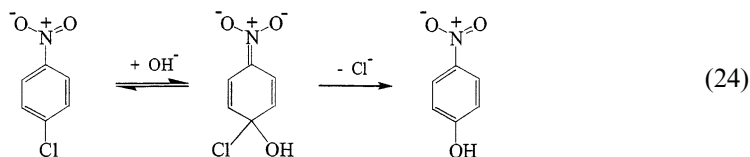
arene prior to electron transfer and no such (reactive) complexes have been isolated and characterized by X-ray crystallography.

### 3.2. Nucleophilic–electrophilic umpolung

The vast majority of reactions to functionalize aromatic hydrocarbons is based on *electrophilic* aromatic substitution, i.e. the electron-rich  $\pi$ -system of the arene substrate acts as a Lewis base and is readily attacked by electrophiles (or Lewis acids,  $E^+$ ) such as nitronium, halonium, etc. [94]. Addition of the electrophile to the aromatic ring causes a temporary breakdown of the aromaticity, which is subsequently restored in the deprotonation step (see Eq. (23)).

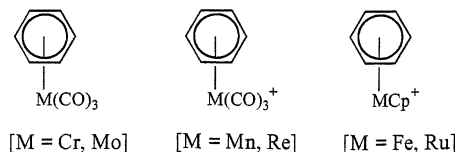


Thus, the addition/deprotonation sequence results in an overall replacement of an aromatic hydrogen (H) by the electrophile (E). Owing to the electron-richness of arenes, *nucleophilic* substitution on the aromatic ring is generally not favored. However, it can be achieved (for example) by attaching both electron-withdrawing substituents (such as nitro, cyano, etc.) and good leaving groups (such as chloro, sulfonato, etc.) to the arene substrate [95]. Both types of substituents together promote nucleophilic substitution via an addition/elimination mechanism (see Eq. (24)).



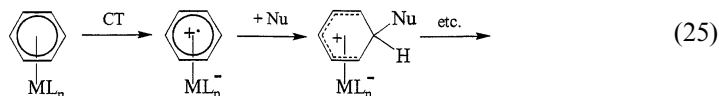
In this reaction sequence, the role of the electron-withdrawing substituent is critical in that it effects electron deficiency on the aromatic ring to such a degree that addition of a nucleophile (e.g.  $OH^-$ ) becomes possible.

Activation of an aromatic substrate for nucleophilic addition can also be achieved by coordination of the arene ring to an electron-withdrawing metal center. In fact, this method is much more effective considering the fact that the electron-acceptor properties of metal complexes can be varied to a much greater extent than those of organic substituents such as nitro or cyano groups. Accordingly, a great variety of organometallic complexes containing arene ligands have been prepared to explore the reactivity of the ligated arene toward nucleophiles [85,96,97]. In this review, we will focus on a few striking examples that illustrate nucleophilic reactivity of aromatic ligands in metal–arene complexes of the following general formulae (see Scheme 15):



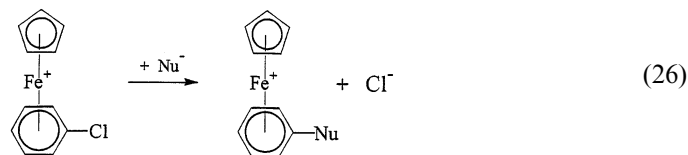
Scheme 15.

We will show that the well-known effect of nucleophilic–electrophilic *umpolung* of metal-ligated arenes can be readily explained by strong charge-transfer interactions between the arene ligand and the metal center. This is best demonstrated in the extreme case of complete electron transfer from the arene to the metal which leads to the generation of an aromatic cation radical that readily reacts with a variety of nucleophiles [98–102] (see Eq. (25)).

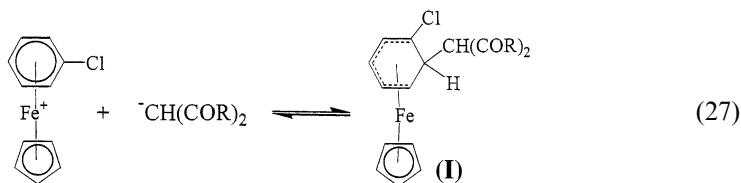


In general, nucleophilic–electrophilic *umpolung* of metal-ligated arenes can lead to four types of reactions: (i) nucleophilic addition; (ii) nucleophilic substitution; (iii) electron transfer; and (iv) proton elimination/transfer. The latter reaction pathway is already discussed in the previous section on carbon–hydrogen bond activation, which shows that C–H bond activation and electrophilic–nucleophilic *umpolung* of metal-ligated arenes are closely related and frequently concomitant processes.

In addition to the coordination of the arene to an electron-withdrawing metal center, nucleophilic substitution also requires suitable leaving groups on the arene ligand (vide supra). Moreover, the reactivity of arene ligands towards nucleophiles in (arene)ML<sub>n</sub> complexes depends on the electrophilicity of the metal fragment [ML<sub>n</sub>], e.g. [Cr(CO)<sub>3</sub>] < [Mo(CO)<sub>3</sub>] << [FeCp]<sup>+</sup> < [Mn(CO)<sub>3</sub>]<sup>+</sup> [85,119]. Among these systems, (arene)FeCp<sup>+</sup> [103] and (arene)RuCp<sup>+</sup> [104] complexes are most intensively studied and most frequently exploited for synthetic purposes. For example, [(C<sub>6</sub>H<sub>5</sub>Cl)FeCp]<sup>+</sup> readily reacts with various nucleophiles (Nu<sup>−</sup>) such as amides, enolates, thiolates, alkoxides, and carbanions [103,105] (see Eq. (26)).

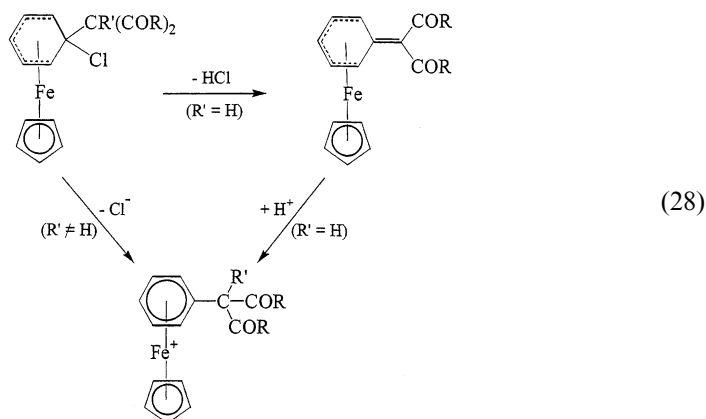


The chloro group in the arene ligand is frequently replaced by a nitro group, which is similarly suitable as a leaving group [106–108]. It is generally believed that the addition of the nucleophile occurs initially in the *ortho*-position with respect to the leaving group. In fact, in the reaction of [(C<sub>6</sub>H<sub>5</sub>Cl)FeCp]<sup>+</sup> with relatively stable carbanions such as CH(COR)<sub>2</sub><sup>−</sup>, the *ortho* addition product **I** can be isolated [109,110] (see Eq. (27)).

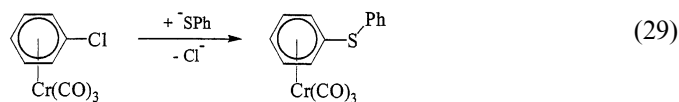




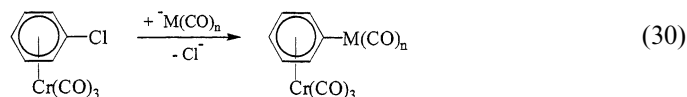
However, subsequent migration of the nucleophile may result in the formation of the *ipso* adduct which then either loses hydrochloride or chloride (if the nucleophile cannot be deprotonated [111] (see Eq. (28)).



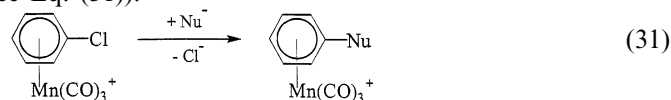
Similar reaction mechanisms have been formulated for substitution reactions involving (arene)Cr(CO)<sub>3</sub> or (arene)Mn(CO)<sub>3</sub><sup>+</sup> complexes. For example, fluoro- or chloro-substituted (arene)Cr(CO)<sub>3</sub> complexes react with nucleophiles such as carbanions [112], amines [113,114] or thiolates [114–116] (see Eq. (29)).



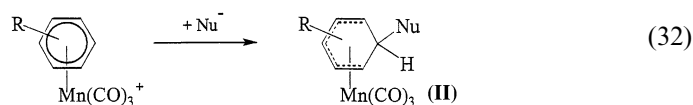
The use of organometallic nucleophiles such as carbonyl metallates M(CO)<sub>n</sub><sup>-</sup> (M = Fe [117], W [118], etc.) leads to the formation of bimetallic complexes (see Eq. (30)).



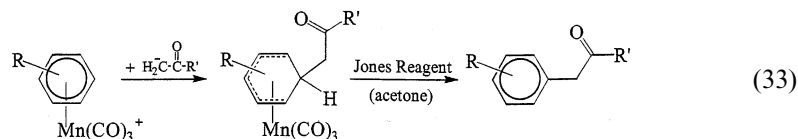
Less substitution reactions are known with (arene)Mn(CO)<sub>3</sub><sup>+</sup> complexes. However, the synthetically useful reactions of (chlorobenzene)Mn(CO)<sub>3</sub><sup>+</sup> with various nucleophiles such as methoxide, benzenethiolate, azide, various amines and anilines [119] need to be mentioned (see Eq. (31)).



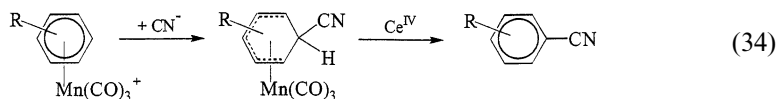
On the other hand, (arene)Mn(CO)<sub>3</sub><sup>+</sup> complexes have been extensively studied for nucleophilic *addition* reactions resulting in thermally stable cyclohexadienyl complexes [96] (see Eq. (32)).



Grignard reagents and enolates are especially suitable for such nucleophilic additions [120]. The resulting addition products (**II**) are of great synthetic interest since treatment with an oxidant (such as chromic acid/ sulfuric acid, Jones reagent) leads to a rapid release of the metal group, and free, functionalized arenes are readily obtainable [120] (see Eq. (33)).



Similarly, benzonitriles can be prepared by addition of cyanide to the corresponding (arene) $\text{Mn(CO)}_3^+$  complex followed by oxidation with ceric sulfate [121] (see Eq. (34)).



It has been emphasized that additions of nucleophiles to  $(\text{arene})\text{Mn(CO)}_3^+$  complexes do *not* occur via an initial electron transfer from the nucleophile to the metal center [96]. This represents an additional advantage since such redox reactions frequently lead to decomposition of the metal complex. A typical example is the reductive deligation of *bis*(arene) $\text{Fe}^{2+}$  complexes [66]. On the other hand, there are other electron donor–acceptor interactions to be pointed out, which are crucial for efficient nucleophilic additions/substitutions, viz. the intramolecular charge transfer from the arene ligand to the electrophilic metal center. These charge-transfer interactions not only effect electron deficiency on the arene ring, which — as in nucleophilic aromatic substitutions (*vide supra*) — is critical for effective attack by a nucleophile, but also result in an attenuation of the electrophilicity of the metal center which prohibits undesired electron-transfer reactions of the metal with the nucleophile (as observed for example with *bis*(arene) iron(II) complexes [66]). In its extreme case, complete electron transfer from the arene ligand to the metal center takes place (see Eq. (25)), which generates an aromatic cation radical (which readily reacts with various nucleophiles [98–102]) and a negatively-charged metal group (which cannot easily be further reduced). The nucleophilic adduct in Eq. (25) can subsequently regain aromaticity by oxidation.

#### 4. $\eta^1$ - and $\eta^2$ -Coordinated arene ligands

The following section will describe structural and electronic effects in  $\eta^1$ - and  $\eta^2$ -coordinated metal–arene complexes in more detail. First, we need to emphasize that the topological classification of metal–arene complexes in terms of hapticity which was originally proposed by Cotton in 1968 [122] as the basis to distinguish organometallic complexes and their chemistry, was never intended to characterize

the chemical bonding between metal and ligands. In fact, the hapticity concept was introduced to ‘avoid implications and, hence, subjective judgments about bonding details’ [122] which leads to both advantages and disadvantages in understanding organometallic chemistry. Most importantly, we need to distinguish between formal electron count and actual electron distribution or — in other terms — between donor–acceptor bonding based on formal metal–ligand coordination or based on actual charge transfer. Moreover, we note that there is no strict correlation between the number of carbon atoms (of the ligand) closest to the metal center and the number of electrons supplied by metal and ligand to form bonds. In other words, the number of electrons formally ‘donated’ by the ligand to provide an 18- or 16-electron environment for the metal (according to the valence-bond description of the complex [6]) does not necessarily correspond to the actual number of bonding electrons and does not take into account any charge-transfer interactions (of varying degree and direction) between metal and ligand.

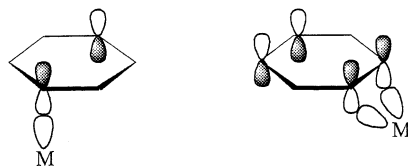
For example, the hapticity concept considers the benzene molecule as a ligand with six carbon atoms equally accessible for metal coordination, which explains the existence of metal–arene complexes of various ( $\eta^1$  through  $\eta^6$ ) coordinations. Moreover, the MO scheme of benzene exhibits six electrons in its upper delocalized  $\pi$ -bonding orbitals, which are equally available for bond formation. In fact, the vast majority of metal–arene complexes exhibit  $\eta^6$ -coordination with equal metal–carbon distances and equal contribution of all  $\pi$ -orbitals to the coordination bonding. In contrast, arene ligands of lower hapticity ( $\eta^1$  through  $\eta^5$ ) exhibit aromatic  $\pi$ -orbitals that are no longer equivalent. As a consequence, the orbital symmetry of the benzene ring is distorted up to the point of complete loss of aromaticity, and the arene ligand becomes very reactive due to an energy level of about 40 kcal mol<sup>−1</sup> higher than that of the resonance-stabilized free arene [123,124]. Needless to say that such reactive complexes are difficult to isolate and to study by X-ray crystallography, and many structural data are still not available or of low precision. However,  $\eta^1$  and  $\eta^2$  complexes represent the most interesting substrates to study the nature of metal–ligand bonding since charge-transfer effects are more pronounced than those in complexes of higher hapticity.

Although there is a large difference between  $\eta^1$  and  $\eta^2$  complexes from the structural point of view, their electronic configurations are closely related since (i) in both types of complexes two electrons are involved in the coordination bonds, and (ii) facile interconversion between the two coordination types is frequently observed. The latter phenomenon is readily explained by considering the MO scheme of benzene [125] with two degenerate HOMOs ( $1E_{1g}$ -A and  $1E_{1g}$ -B) (see Scheme 16).



Scheme 16.

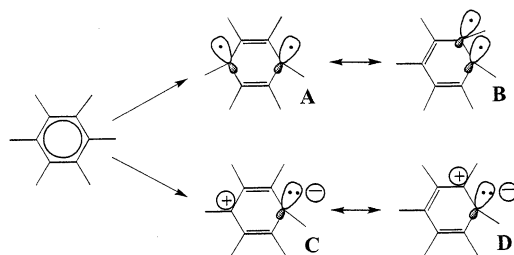
Thus, the two-center MO  $1E_{1g}$ -A is suitable for  $\eta^1$ -coordination whereas the four-center MO  $1E_{1g}$ -B provides better conditions for  $\eta^2$ -coordination (see Scheme 17).



Scheme 17.

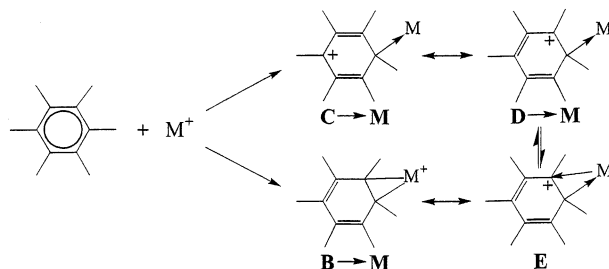
Although the initial energies of orbitals A and B are equal,  $\eta^1$ - and  $\eta^2$ -coordination are usually not equally favored mainly due to charge-transfer effects which are not equivalent for both coordination types.

The relationship between  $\eta^1$ - and  $\eta^2$ -coordination is even more clearly visualized by traditional resonance schemes. For example, two-electron coordination results in two sets of resonance structures including either biradical or bipolar forms (see Scheme 18).



Scheme 18.

All four resonance structures have two (localized) double bonds in common, however the different locations of the two bonding electrons lead to preferences between  $\eta^1$ - and  $\eta^2$ -coordination. The bipolar resonance structures C and D favor  $\eta^1$ -coordination, whereas structure B is definitely ideal for  $\eta^2$ -coordination (see Scheme 19).



Scheme 19.

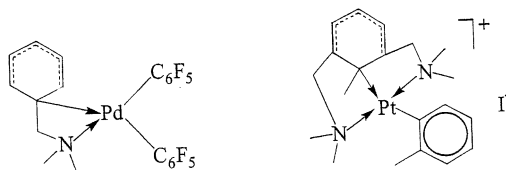
Accordingly,  $\eta^1$ -coordination leads to a polarization of the  $\pi$ -electrons of the aromatic ligand, whereas  $\eta^2$ -coordination does not necessarily lead to polar electronic

configurations. As a consequence, the polarized structures ' $C \rightarrow M$ ' and ' $D \rightarrow M$ ' are expected to predominate in complexes containing metals and arene ligands of very different donor and acceptor strengths, whereas similar donor–acceptor strength of metal and arene ligand will result in structure ' $B \rightarrow M$ ' which is in resonance with ' $E$ '.

Both theoretical description of  $\eta^1$ - and  $\eta^2$ -coordination, viz. in terms of MO orbitals or resonance structures, lead to the same conclusions: (i) the preference of  $\eta^1$ - over  $\eta^2$ -coordination highly depends on the relative donor and acceptor strengths of arene ligand and metal center; and (ii) resonance structure ' $E$ ' allows facile interconversion between the two coordination types. In the following section, we will show that both predictions are verified by numerous examples.

In various series of complexes between organic, inorganic, or organometallic acceptors (or Lewis acids) with arene donors (or Lewis bases), we note a transition from  $\eta^2$ - to  $\eta^1$ -coordination with increasing acceptor strength of the Lewis acid.  $\eta^2$ -Coordination is most frequently observed with weak acceptors. For example, the molecular complex between durene and carbon tetrabromide ( $CBr_4$ ) as the  $\sigma$ -acceptor exhibits a bridging bromine atom between to neighboring ring carbons of durene with carbon–bromine distances of 3.26 and 3.34 Å [25]. Moreover, most of the silver(I) complexes with arenes exhibit bridging positions of  $Ag^+$  between two carbon atoms with equal  $Ag^+ - C$  distance of about 2.5 Å [26,37]. Moderately stronger acceptors such as  $Cu^+$ ,  $Ni^0$ ,  $Hg^{2+}$ , etc. still prefer  $\eta^2$ -coordination. Typical examples are the  $\mu$ - $\eta^2$  complexes of copper(I) [33] and nickel(0) [32] with benzene in which the bridging metals show almost equal distance to the two closest carbon atoms in the aromatic ring ( $d = 2.081$  and  $2.105$  Å [33] and  $d = 2.005$  and  $2.021$  Å [32], respectively). In the  $Hg^{2+} - HMB$  complex [42], the mercury ion is centered over the coordinating carbon–carbon bond with  $Hg - C$  distances of 2.56 and 2.58 Å.  $\eta^2$ -Coordination is also frequently observed in transition-metal complexes of condensed aromatics (such as naphthalene or anthracene) which contain partially localized double bonds ('predisposed' for such coordination, vide infra).

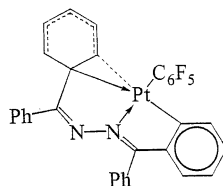
In contrast, strong electron acceptors such as  $Al(C_6F_5)_3$  [39],  $SiEt_3^+$  [38],  $Br^+$  [40], and  $Cl^+$  [41] form exclusively  $\eta^1$ -coordinated arene complexes. Similarly, strong organometallic acceptors such as perfluoroaryl-coordinated Pd(II) or Pt(II) form mostly  $\eta^1$ -arene complexes, where the terminal  $\eta^1$ -coordination results in Pd–C or Pt–C distances which are only about 0.3 Å longer than the carbon–metal  $\sigma$ -bonds between the perfluoroaryl ligands and the metal center (viz.  $d = 2.335$  versus  $2.022$  Å in the Pd complex [126] and  $d = 2.293$  versus  $2.005$  Å in the Pt complex [35]) (see Scheme



Scheme 20.

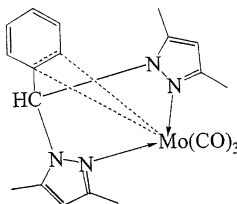
20). Steric hindrance does not seem to have a strong effect on the coordination type. For example, in the (less hindered) Pt complex, which was originally classified as an  $\eta^2$ -coordinated complex [127], the Pt–C(*ipso*) bond is much shorter

( $d_{\text{ipso}} = 2.327 \text{ \AA}$ ) than the adjacent Pt–C(*ortho*) bond ( $d_{\text{ortho}} = 2.610 \text{ \AA}$ ) which reveals the true  $\eta^1$ -coordination of the platinum(II) atom (see Scheme 21). Most impor-



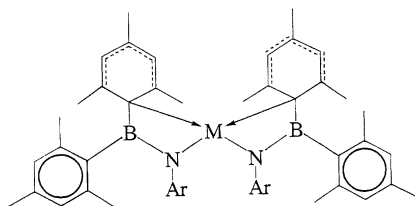
Scheme 21.

tantly, in a similar complex with the weaker acceptor  $\text{Mo}(\text{CO})_3$ , an almost symmetrically bridged Mo atom with clear  $\eta^2$ -coordination is observed ( $d_{\text{Mo-C}} = 2.776(4)$  and  $2.840(4) \text{ \AA}$  for *ipso*- and *ortho*-coordination, respectively [28]) (see Scheme 22).



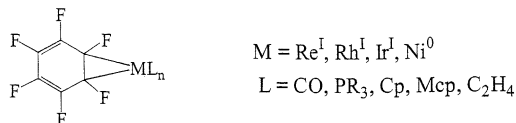
Scheme 22.

A comparison of complexes consisting of organometallic acceptors (Lewis acids) of comparable acceptor strength and arenes (Lewis bases) of various donor or acceptor strengths reveals very similar effects of the relative donor–acceptor strength of metal and arene on the coordination type. Thus, with increasing acceptor strength of the arene Lewis bases a transition from  $\eta^1$ - to  $\eta^2$ -coordination is observed. For example, complexes of bivalent d-metals (from Cr(II) to Ni(II)) show  $\eta^1$ -coordinated mesityl groups [34] (see Scheme 23).



Scheme 23.

In contrast, Re(I), Rh(I), Ir(I), and Ni(0) metal centers form  $\eta^2$ -coordinated complexes with the electron acceptor hexafluorobenzene acting as a Lewis base [43] (see Scheme 24).

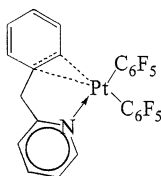


Scheme 24.

The general rule that strong charge-transfer bonding leads to  $\eta^1$ -coordination and weak donor–acceptor interactions result in  $\eta^2$ -coordination is not always applicable. In energetic terms, charge-transfer interactions may shift the relative energy levels of  $\eta^1$ - and  $\eta^2$ -coordinated isomers, but both isomers will still remain very close in energy. As a result, even the strongest  $\eta^1$ -complexes such as chloroare-nium ( $\text{Ar(H)Cl}^+$ ) [129] or the strongest  $\eta^2$ -complexes such as hexafluorobenzene–metal complexes [43] exhibit fast  $\eta^1$ – $\eta^2$  interconversion in solution<sup>5</sup> as revealed by NMR spectroscopy. Only at low temperature, the more stable isomer predominates. Similarly, crystallization processes generally produce the more stable isomer, although crystal packing factors may lead to the less stable isomers in some cases. Such exceptions further confirm the close energetics and interconvertability of  $\eta^1$ - and  $\eta^2$ -coordination.

There are a few exceptions known that deviate from the generally observed  $\eta^2$ -coordination of silver(I) with arenes [37].  $\eta^1$ -Coordination forced by steric effects is observed with some Cu(I) complexes [36]. Moreover, an asymmetric position of the  $\eta^2$ -coordinated cobalt in the  $[\text{Co}(\text{anthracene})(\text{PMe}_3)_3]$  complex is found with Co–C distances of 2.036 and 2.096(9) Å [47], which is highly unusual for metal complexes with condensed arenes that generally exhibit symmetric  $\eta^2$ -coordination.

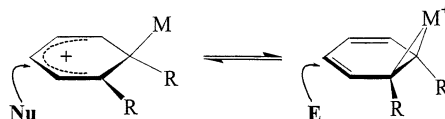
On the other hand, there is at least one example of an unusual  $\eta^2$ -coordination of generally  $\eta^1$ -coordinated perfluorarene–Pt(II) complexes with Pt–C distances of 2.363 and 2.375(7) Å [29] (see Scheme 25).



Scheme 25.

Interestingly, the coexistence of  $\eta^1$ - and  $\eta^2$ -coordinated metal–arene complexes in solution (*vide supra*) results in a dual reactivity of the isomers toward electrophiles and nucleophiles. The  $\eta^1$ -coordinated isomer with a high degree of charge transfer exhibits a more polarized structure with a positive charge residing on the benzene ring which leads to enhanced reactivity toward nucleophiles and/or deprotonation. In contrast, the  $\eta^2$ -coordinated isomer exhibits high electron density (negative charge) at the localized double bonds and is hence subject to electrophilic attack (see Scheme 26).

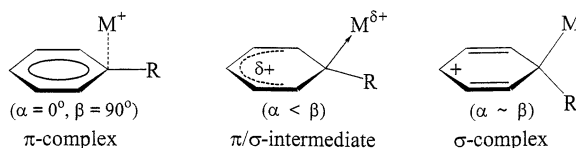
<sup>5</sup> The only complex — to our knowledge — which exhibits an equilibrium between  $\eta^1$ - and  $\eta^2$ -coordination in the crystalline state is  $[(t\text{-Bu}_3\text{SiO})_3\text{Ta}]_2(\mu\text{-C}_6\text{H}_6) \cdot 2\text{C}_6\text{H}_6$  [128]. The X-ray structure shows the benzene ligand rotationally disordered between the two Ta(III) centers. Presumably, the disorder is caused by rapid interconversion between  $\mu\text{-}\eta^1(1):\eta^1(4)$ - and  $\mu\text{-}\eta^2(1,2):\eta^2(4,5)$ -coordinated species.



Scheme 26.

It is important to note that such equilibria between the two coordination types and the related electrophilic versus nucleophilic reactivity can be shifted completely to one or the other side by changing the relative donor–acceptor strengths of the complex partners.

Significant changes in structure and chemical reactivity can also be achieved within one coordination type due to varying degrees of charge-transfer bonding. For example, in  $\eta^1$  complexes of arene ligands with Lewis acids of increasing acceptor strength, a continuous transition from  $\pi$  to  $\sigma$  coordination is observed which is established by the structural features (bond lengths and angles) in Table 3 [12,34–36,38–40,127,130–135] (see Scheme 27).



Scheme 27.

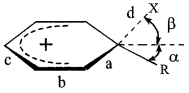
The  $\pi \rightarrow \sigma$  transition is accompanied by several structural changes. (i) Shortening of the distance between Lewis acid and *ipso*-carbon atom of the arene from van der Waals contact to covalent bond. (ii) Deviation of the *ipso*-substituent out of the plane of the aromatic ring, which corresponds to an increase in the  $\alpha$  angle from 0 to  $55^\circ$  and an decrease in the  $\beta$  angle from 90 to  $55^\circ$ . The changes in the angles are due to the transition from  $sp^2$  to  $sp^3$  hybridization. (iii) Redistribution of bond lengths in the benzene ring, viz. elongation of the 1,2-bond up to the standard distance of  $d = 1.50 \text{ \AA}$  for a  $C(sp^2)–C(sp^3)$  single bond as well as partial localization of the 2,3-double bond. (iv) Complete charge transfer from the aromatic ring to the Lewis acid resulting in a positive charge that resides on the aromatic ring.

The structural data presented in Table 3 (in approximate order of increasing X–Ar interaction) cover the entire range of donor–acceptor interactions between Lewis acids and arenes — from the weak  $\pi$ -complexes of  $Ag^+$ ,  $Cu^+$ ,  $Ni(II)$ , and  $Al(III)$  to stronger  $\pi$ -complexes with  $Co(II)$ ,  $Si(IV)^+$ , and  $Cr(II)$ , to intermediate ( $\pi/\sigma$ ) complexes of  $Pt(II)$ , and to pure  $\sigma$ -complexes with  $Br^+$  and heptamethylbenzenium.

The localization of the positive charge on the aromatic ring in  $\eta^1$ -coordinated  $\sigma$ -complexes is readily revealed by the distances to the weakly nucleophilic counter anions. For example, the bromohexamethylbenzenium structure (see Section 2.5) shows a shortened carbon–fluorine distance of  $d = 3.066 \text{ \AA}$  (which is  $0.1 \text{ \AA}$  shorter than the van der Waals distance) between one fluorine atom of the  $SbF_6$  counter anion and the carbon in *para*-position relative to the coordination site of bromine



Table 3

Average geometrical parameters ( $\text{\AA}/^\circ$ ) of  $\eta^1$ -coordinated arene complexes


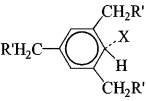
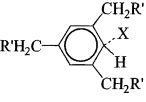
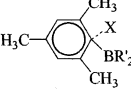
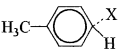
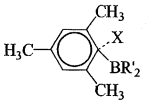
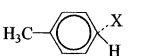
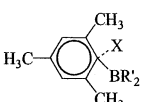
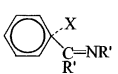
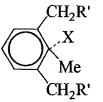
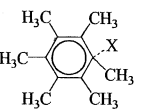
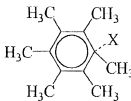
| No. | Arene <sup>a</sup>  | X                                   | $d(d_1)^b$        | $d-d_1$ | $\alpha/\beta$ | a     | b     | c     | Reference |
|-----|---|-------------------------------------|-------------------|---------|----------------|-------|-------|-------|-----------|
| 1.  |    | $\text{Ag}^+$                       | 2.556<br>(~2.10)  | 0.46    | 3/83.3         | 1.399 | 1.387 | 1.393 | [36,130]  |
| 2.  |    | $\text{Cu}^+$                       | 2.391<br>(~1.96)  | 0.43    | 7/75.5         | 1.398 | 1.393 | 1.391 | [36,131]  |
| 3.  |    | $\text{Ni}^{\text{II}}$             | 2.386<br>(~1.98)  | 0.41    | 6/68           | 1.42  | 1.39  | 1.39  | [34,132]  |
| 4.  |    | $\text{Al}(\text{C}_6\text{F}_5)_3$ | 2.366<br>(~1.98)) | 0.39    | 9/84.1         | 1.403 | 1.388 | 1.391 | [39,133]  |
| 5.  |    | $\text{Co}^{\text{II}}$             | 2.387<br>(~2.06)  | 0.33    | 6/66           | 1.42  | 1.38  | 1.38  | [34,132]  |
| 6.  |    | $\text{SiEt}_3^+$                   | 2.187<br>(~1.888) | 0.30    | 8/76.0         | 1.408 | 1.372 | 1.379 | [12,38]   |
| 7.  |   | $\text{Cr}^{\text{II}}$             | 2.377<br>(~2.10)  | 0.28    | 9/62           | 1.41  | 1.39  | 1.37  | [34,134]  |
| 8.  |  | $\text{Pt}^{\text{II}}$             | 2.327<br>(~2.148) | 0.18    | 17/81          | 1.40  | 1.43  | 1.38  | [127,132] |
| 9.  |  | $\text{Pt}^{\text{II}}$             | 2.293<br>(2.148)  | 0.14    | 22/79          | 1.40  | 1.39  | 1.36  | [35,132]  |
| 10. |  | $\text{Br}^+$                       | 2.006<br>(1.966)  | 0.04    | 42.4/67.1      | 1.496 | 1.375 | 1.428 | [12,40]   |

Table 3 (Continued)

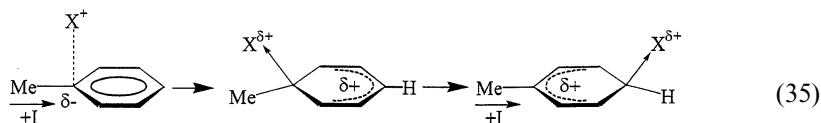
|     |   |                 |                               |      |           |       |       |       |          |
|-----|---|-----------------|-------------------------------|------|-----------|-------|-------|-------|----------|
| 11. |  | Me <sup>+</sup> | 1.564<br>(1.534) <sup>b</sup> | 0.03 | 55.3/55.3 | 1.493 | 1.375 | 1.423 | [12,135] |
|-----|---|-----------------|-------------------------------|------|-----------|-------|-------|-------|----------|

<sup>a</sup> Note that the arenes are formally represented as aromatic systems although the degree of aromaticity varies substantially — depending on the substrate — from an almost unperturbed (6 $\pi$ -delocalized) to a cyclohexadienyl (5 $\pi$ -delocalized) electronic configuration.

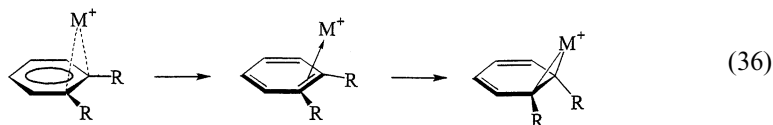
<sup>b</sup>  $d_1$  is a standard value (or an estimate) for the length of a single  $\sigma$ -bond C(sp<sup>3</sup>)-X.

[40]. Most importantly, the methyl group on the *para*-carbon atom is bent away from the interacting fluorine atom by 6.3° relative to the aromatic plane. Similarly, heptamethylbenzenium co-crystallized with the relatively strong nucleophilic AlCl<sub>4</sub><sup>−</sup> counter anion shows short contacts ( $d = 3.306$  and  $3.323$  Å as compared to the van der Waals distance of  $3.45$  Å) between two chlorine atoms of the counter anion and the carbon atom in *para*-position to the sp<sup>3</sup>-hybridized carbon [135]. Interestingly, the crystal structure of [C<sub>6</sub>Me<sub>6</sub>Br<sup>+</sup>]<sup>+</sup>Br<sub>3</sub><sup>−</sup>·Br<sub>2</sub> [136] exhibits infinite parallel stacks of positively charged aromatic rings and neutral dibromine molecules with an intermolecular distance of  $3.55$  Å. These alternate stacks are reminiscent of the donor–acceptor stacking in organic donor–acceptor ( $\pi$ ) complexes.

In  $\eta^1$  complexes of lower degrees of charge transfer, less positive charge is localized on the aromatic ring, however a polarization of the benzene ring is frequently observed. For example, the crystal structures of the weak complexes of Al(C<sub>6</sub>F<sub>5</sub>)<sub>3</sub> and SiEt<sub>3</sub><sup>+</sup> with toluene reveal that the Lewis acid does not approach the *ipso*-carbon which is presumably the most electron-rich center, but the carbon in *para*-position to the methyl group. As a result, the partial positive charge generated by the coordination of the Lewis acid is mainly located at the methyl-substituted carbon atom and thus best stabilized by the donor properties of the methyl substituent. However, it is generally assumed that the initial electrophilic attack of the Lewis acid occurs on the (methyl-substituted) *ipso*-carbon. Subsequently, the positive charge on the arene ring is stabilized by migration of the Lewis acid to the *para*-carbon atom (Eq. (35)).



$\eta^2$ -Coordination in metal–arene complexes is only observed with relatively weak electron acceptors, since strong donor–acceptor complexes tend to prefer  $\eta^1$ -coordination (vide supra). Typical examples include  $\eta^2$ -arene/Ag<sup>+</sup> complexes a series of which has been structurally characterized. Although subtle structural changes in the benzene ring upon coordination to the metal center cannot be revealed — owing to the low precision of most of these crystal structures — some trends in the structures can be recognized which depend on the electron-acceptor properties of the metal. Thus, with increasing acceptor strength a transition from weak  $\pi$  coordination to  $\sigma$  coordination is observed (Eq. (36)), which is accompanied by



several structural changes as follows: First, the distance between the metal and the two coordinated carbon atoms of the benzene ring is shortened from that of a pure van der Waals contact to that of a covalent bond. Second, a deviation of the *ipso*-substituents out of the plane of the benzene ring and away from the metal (approaching the aromatic system from the opposite side) is observed. This structural change is manifested by the changes in the angles  $\alpha$  (from 0 to 60°) and  $\beta$  (from 90 to 60°, see Table 4) [12,25,26,28–33,42,43,61,130–132,137–142] which reveal the re-hybridization of the *ipso*-carbon atoms from  $sp^2$  to  $sp^3$ . Third, the relative bond lengths within the benzene ring change significantly. For example, in  $\pi$  ( $\eta^2$ ) complexes, an elongation of the b- and d-bond and a contraction of the c-bond is observed, whereas the a-bond remains unchanged. In contrast,  $\sigma$  ( $\eta^2$ ) complexes exhibit strongly elongated b-, d-, and a-bonds up to the length of a carbon–carbon single bond and the c-bond is contracted to the length of a C–C double bond.

In very weak  $\pi(\eta^2)$ -coordinated complexes, no significant changes in the geometry of the arene ligand can be detected. Moreover, a bridging arene position between two acceptors is frequently observed which leads to  $\mu\text{-}\eta^2$  (1,2):(4,5) complexes (see entries 1 and 2 in Table 4), in which two acceptors compete for the same four-center  $1E_{1g}$ -HOMO of the benzene ligand (*vide supra*). As a result, potential structural effects would not be noticeable since the two metal centers cause opposite changes in the geometry of the benzene ring which annihilate each other. Fortunately, a few non-bridged  $\text{Ag}^+$ /arene complexes are known with sufficiently precise crystal structures that allow the observation of an incipient double-bond localization in the benzene ring due to  $\eta^2$ -coordination (see entry 3 in Table 4). In another example, viz.  $\text{Hg}^{2+}$ /HMB complex (see entry 4),  $sp^2/sp^3$  re-hybridization is evident although the limited precision of this crystal structure does not allow the detection of changes in the relative bond lengths in the benzene ring.

Stronger metal acceptors promote more clearly the formation of localized double bonds in the  $\eta^2$ -coordinated benzene ring as illustrated with  $\text{Mo}^0$  and  $\text{Pt(II)}$  complexes (see entries 5 and 6).<sup>6</sup> Localized double-bonds, in turn, represent attractive targets for further attack by a second electrophilic center which explains the frequent observation of  $\mu\text{-}\eta^2(1,2):\eta^2(3,4)$  complexes such as described in entries 7 through 10. Most importantly, the (1,2):(3,4) coordination results in *cumulative* effects on the geometry of the benzene ring and the strength of the metal–carbon bond — as opposed to the *annihilating* effects in (1,2):(4,5)-coordinated complexes (*vide supra*). For example, the Cu–C and the Ni–C bond distances in the  $\mu\text{-}\eta^2(1,2):\eta^2(3,4)$  complexes (entries 7 and 8 in Table 4) are even shorter than the

<sup>6</sup> Note that  $\text{Pt(II)}$  complexes already show a preference for  $\eta^1$ -coordination (*vide supra*).

metal–carbon bond distances in the corresponding  $\eta^1$ -coordinated complexes (see entries 2 and 3 in Table 3), although in general,  $\eta^2$ -coordination is weaker than  $\eta^1$ -coordination (in unbridged complexes).<sup>7</sup> In fact,  $\mu\text{-}\eta^2(1,2):\eta^2(3,4)$  coordination in the  $\text{Ni}^0$  complex results in metal–carbon distances very close to a single  $\sigma$  bond (see entry 8 in Table 4).<sup>8</sup>

In general,  $\eta^2$ -coordination of an arene to a metal center is favored if the double bonds in the benzene ring are already partially localized as demonstrated with the  $\mu\text{-}\eta^2(1,2):\eta^2(3,4)$  coordinated complexes. Partial double-bond localization is also present in condensed aromatic systems such as naphthalene or anthracene even in the uncoordinated state [143,144]. This is illustrated with two examples (see entries 11 and 12 in Table 4) for which the crystallographic data are sufficiently precise to reveal the structural effects of  $\eta^2$ -coordination. The metal–carbon distances in these two examples are very close to those of metal–carbon  $\sigma$  bonds and the C–C bond distances are close to those of localized C–C double bonds. Moreover, the  $\text{Ru}(\text{I})$  complex (entry 11) exhibits a severe distortion of the planarity of the benzene ring.<sup>9</sup> The structural effects in the  $\text{Ni}(0)$ –naphthalene complex are comparable to those observed with the  $\mu\text{-}\eta^2(1,2):\eta^2(3,4)$  coordinated  $\text{Ni}(0)$ –benzene complex (compare entries 8 and 12 in Table 4). As an example of double coordination of naphthalene with two metal centers, the rhodium(I) complex  $[(\text{RhMCpPMe}_3)_2\text{C}_{10}\text{H}_8]$  should be mentioned [145].

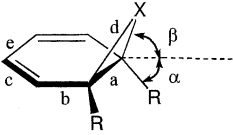
All examples of  $\eta^1$  and  $\eta^2$ -coordination described so far in this section reveal the arene ligand as the Lewis base and electron donor whereas the metal center acts as Lewis acid and electron acceptor. Thus, (formal) two-electron donation and (actual) charge transfer occur in the same direction, viz. from the arene to the metal. However, other scenarios are conceivable in which coordination and charge transfer are in fact of opposite direction. For example, the arene ligand may act as Lewis base for coordination to a coordinatively unsaturated metal center, but subsequently withdraws electrons from the metal due to its high electron-acceptor strength relative to that of the metal. A typical case is hexafluorobenzene (HFB), which donates two electrons for coordination to a metal center. However, the metal/HFB complex exhibits substantial (back-) charge transfer from the metal to the arene which results in the formation of a strong  $\sigma$  ( $\eta^2$ ) complex (see entries 13 through 16 in Table 4).  $\eta^1$ -coordination is not favored in these cases since it would leave a positive charge on an already electron-deficient benzene ring; however,  $\eta^1$ – $\eta^2$  interconversion has been observed at higher temperatures [43]. Many examples of such complexes are known with metals of medium donor–acceptor properties, which enable them to coordinate efficiently with both donor and

<sup>7</sup> Compare, for example,  $\eta^1$ - and  $\eta^2$ -coordinated  $\text{Pt}(\text{II})$  complexes (entries 8 and 9 in Table 3 and entry 6 in Table 4).

<sup>8</sup> This is also presumably true for  $\text{Re}(\text{I})$  and  $\text{Os}(\text{II})$   $\mu\text{-}\eta^2(1,2):\eta^2(3,4)$  complexes (see entries 9 and 10 in Table 4). Unfortunately, the crystal structures are not precise enough to prove this point.

<sup>9</sup> The degree of distortion in the  $\text{Ni}(0)$  complex (entry 12) is unclear since the coordinates of the hydrogen atoms are not available.

Table 4

Average geometrical parameters (Å/°) of  $\eta^2$ -coordinated arene complexes


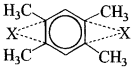
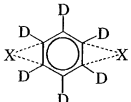
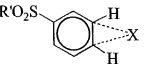
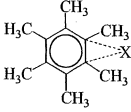
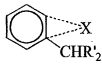
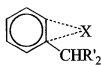

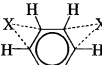
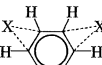
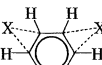
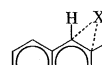
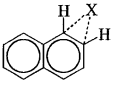
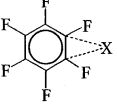
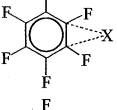
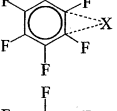
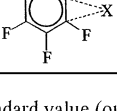
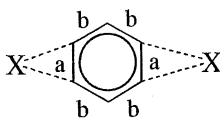
| No. | Arene   | X                     | d(d <sub>1</sub> ) <sup>a</sup> | d-d <sub>1</sub> | α/β                  | a     | b     | c     | e                  | Reference |
|-----|---|-----------------------|---------------------------------|------------------|----------------------|-------|-------|-------|--------------------|-----------|
| 1.  |    | Br(CBr <sub>3</sub> ) | 3.299<br>(1.966)                | 1.33             | 0.1/87.0             | 1.411 | 1.399 | -     | - <sup>b</sup>     | [12,25]   |
| 2.  |    | Ag <sup>+</sup>       | 2.565<br>(~2.10)                | 0.46             | 4/78                 | 1.405 | 1.398 | -     | - <sup>b</sup>     | [26,130]  |
| 3.  |    | Ag <sup>+</sup>       | 2.580<br>(~2.10)                | 0.48             | 2/72.5               | 1.387 | 1.392 | 1.379 | 1.392              | [130,137] |
| 4.  |    | Hg <sup>2+</sup>      | 2.567<br>(~2.12)                | 0.45             | 4/94                 | 1.43  | 1.42  | 1.41  | 1.39               | [42,132]  |
| 5.  |    | Mo <sup>0</sup>       | 2.802<br>(~2.41)                | 0.39             | 6/72.3               | 1.402 | 1.395 | 1.369 | 1.378              | [28,132]  |
| 6.  |   | Pt <sup>II</sup>      | 2.369<br>(2.148)                | 0.22             | 14/76.5              | 1.400 | 1.416 | 1.349 | 1.408              | [29,132]  |
| 7.  |  | Cu <sup>+</sup>       | 2.137<br>(~1.96)                | 0.18             | 11/78.7              | 1.404 | 1.414 | 1.374 | 1.427 <sup>c</sup> | [33,131]  |
| 8.  |  | Ni <sup>0</sup>       | 2.013<br>(~1.98)                | 0.03             | 21/75.3              | 1.421 | 1.451 | 1.340 | 1.474 <sup>c</sup> | [32,132]  |
| 9.  |  | Re <sup>I</sup>       | 2.269<br>(~2.22)                | 0.04             | - <sup>d</sup> /65.2 | 1.40  | 1.46  | 1.31  | 1.47 <sup>c</sup>  | [138,139] |
| 10. |  | Os <sup>2+</sup>      | 2.185<br>(~2.13)                | 0.05             | - <sup>d</sup> /69.7 | 1.46  | 1.49  | 1.32  | 1.51 <sup>c</sup>  | [140,141] |
| 11. |  | Ru <sup>I</sup>       | 2.208<br>(~2.145)               | 0.06             | 29/65                | 1.418 | 1.426 | 1.346 | 1.432 <sup>a</sup> | [30,132]  |

Table 4 (Continued)

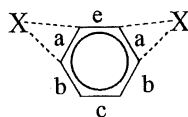
|     |   |                 |                  |       |                      |       |       |       |                    |           |
|-----|---|-----------------|------------------|-------|----------------------|-------|-------|-------|--------------------|-----------|
| 12. |  | Ni <sup>0</sup> | 1.995<br>(~1.98) | 0.02  | - <sup>d</sup> /79.0 | 1.436 | 1.427 | 1.344 | 1.445 <sup>e</sup> | [31,132]  |
| 13. |  | Rh <sup>I</sup> | 2.058<br>(2.092) | -0.04 | 43.8/71.4            | 1.40  | 1.47  | 1.33  | 1.35               | [132,142] |
| 14. |  | Ni <sup>0</sup> | 1.944<br>(~1.98) | -0.04 | 44/66                | 1.486 | 1.429 | 1.320 | 1.416              | [32,132]  |
| 15. |  | Re <sup>I</sup> | 2.185<br>(~2.22) | -0.03 | 46.4/65.7            | 1.48  | 1.43  | 1.33  | 1.43               | [43,138]  |
| 16. |  | Ir <sup>I</sup> | 2.07<br>(~2.11)  | -0.04 | 47.9/65.4            | 1.47  | 1.43  | 1.33  | 1.43               | [61,132]  |

<sup>a</sup> d<sub>1</sub> is a standard value (or an estimate) for the length of a single  $\sigma$ -bond C(sp<sup>3</sup>)-X.

<sup>b</sup> Bond labeling in  $\mu$ - $\eta^2(1,2):(4,5)$ -arene ligands:

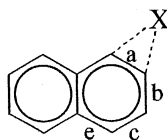


<sup>c</sup> Bond labeling in  $\mu$ - $\eta^2(1,2):(3,4)$ -arene ligands:



<sup>d</sup>  $\alpha$ -angle is not available (see text).

<sup>e</sup> Bond labeling in  $\eta^2$ -naphthalene ligands:



acceptor arene ligands. For example, nickel(0) binds to naphthalene, benzene, and hexafluorobenzene (see entries 12, 8, and 14, respectively). Most revealing are the structural features of the hexafluorobenzene complexes, which exhibit high degrees of charge transfer and consequently high degrees of  $\sigma$  bonding. As a result, the arene ligand shows a clear cyclohexadienyl structure, the fluorine atoms at the *ipso* carbon atoms deviate from the plane of the benzene ring up to an angle of 48°, and the metal–carbon distances are even shorter than those of standard metal–carbon(sp<sup>3</sup>) bonds — as expected for a strained three-membered metal–carbon–carbon ring system.<sup>10</sup>

## 5. Conclusions

In general, crystal structures of organometallic coordination compounds are reported from the metal center's point of view in order to discuss the symmetry of the valence orbitals and the ligand environment. In this review, we examine the X-ray structures of numerous transition metal–arene complexes with the focus on the arene ligand. This alternative approach reveals a series of significant structural details that clearly point to the importance of charge transfer in metal–arene coordination. The resulting concept of charge-transfer bonding is very useful in understanding and predicting the chemical reactivity of metal-coordinated arenes. We conclude that structural examinations from both the metal's and the ligand's point of view are equally important to obtain a complete picture of the correlation between structure and reactivity in organometallic coordination compounds.

## Acknowledgements

We thank the National Science Foundation and the Robert A. Welch Foundation for financial support.

## References

- [1] J.K. Kochi, *Organometallic Mechanisms and Catalysis*, Academic Press, New York, 1978.
- [2] K.H. Dötz, R.W. Hoffmann (Eds.), *Organic Synthesis via Organometallics*, Vieweg, Braunschweig, 1991.
- [3] D. Astruc, *Electron Transfer and Radical Processes in Transition-Metal Chemistry*, VCH, New York, 1995.
- [4] D. Astruc, *Top. Curr. Chem.* 160 (1992) 47.
- [5] S.G. Davies, T.D. McCarthy, in: E.W. Abel, F.G.A. Stone, G. Wilkinson (Eds.), *Comprehensive Organometallic Chemistry II*, vol. 12, Pergamon, Oxford, 1995, p. 1039.

<sup>10</sup> For example, the standard C(sp<sup>3</sup>)–C(sp<sup>3</sup>) bond length of  $d = 1.534$  Å in open-chain alkanes is reduced to  $d = 1.510$  Å in cyclopropane [12].

- [6] L. Pauling, *The Nature of the Chemical Bond*, Cornell University Press, Ithaca, NY, 1960. See also Ref. [8], p. 280.
- [7] F.A. Cotton, *J. Am. Chem. Soc.* 90 (1968) 6230.
- [8] R.S. Mulliken, W.M. Person, *Molecular Complexes*, Wiley, New York, 1969.
- [9] G. Briegleb, *Elektronen-Donator-Acceptor-Komplexe*, Springer, Berlin, 1961.
- [10] M. Tamres, M. Brandon, *J. Am. Chem. Soc.* 82 (1960) 2134.
- [11] L. Pauling, *The Nature of the Chemical Bond*, Cornell University Press, Ithaca, NY, 1960, pp. 255–256.
- [12] F.H. Allen, O. Kennard, D.G. Watson, L. Brammer, A.G. Orpen, R. Taylor, *J. Chem. Soc. Perkin Trans. 2* (1987) S1.
- [13] G.A. Jeffrey, J.R. Ruble, R.K. McMullan, J.A. Pople, *Proc. R. Soc. Lond. Ser. A* 414 (1987) 47.
- [14] J. Hecht, J.K. Kochi, Electronic submission to the Cambridge Structural Database 138870, 2000.
- [15] E.K. Kim, J.K. Kochi, *J. Am. Chem. Soc.* 113 (1991) 4962.
- [16] J. Hecht, R. Rathore, J.K. Kochi, Electronic submission to the Cambridge Structural Database 138871, 2000.
- [17] S.V. Lindeman, E. Bosch, J.K. Kochi, Electronic submission to the Cambridge Structural Database 138872, 2000.
- [18] J. Hecht, J.K. Kochi, Electronic submission to the Cambridge Structural Database 138873, 2000.
- [19] J. Hecht, R. Rathore and J.K. Kochi, Electronic submission to the Cambridge Structural Database 138874, 2000.
- [20] F. Calderazzo, I. Ferri, G. Pampaloni, S. Troyanov, *J. Organomet. Chem.* 518 (1996) 189.
- [21] R.J. Bernhardt, M.A. Wilmoth, J.J. Weers, D.M. LaBrush, D.P. Eyman, J.C. Huffman, *Organometallics* 5 (1986) 883.
- [22] B.P. Byers, M.B. Hall, *Inorg. Chem.* 26 (1987) 2186.
- [23] J.K. Kochi, C.H. Wei, *J. Organomet. Chem.* 451 (1993) 111.
- [24] A.J. Steedman, A.K. Burrell, *Acta Crystallogr. Sect. C* 53 (1997) 864.
- [25] J. Hecht, J.K. Kochi, Electronic submission to the Cambridge Structural Database 138875, 2000.
- [26] R.K. McMullan, T.F. Koetzle, C.J. Fritchie, *Acta Crystallogr. Sect. B* 53 (1997) 645.
- [27] P. LeMagueres, R. Rathore, J.K. Kochi, submitted to *J. Org. Chem.* Electronic submission to the Cambridge Structural Database 138876–138878, 2000.
- [28] K.-B. Shiu, C.-C. Chou, S.-L. Wang, S.-C. Wei, *Organometallics* 9 (1990) 286.
- [29] J.M. Casas, F. Fornies, A. Martín, B. Menjón, *Organometallics* 12 (1993) 4376.
- [30] C.D. Tagge, R.G. Bergman, *J. Am. Chem. Soc.* 118 (1996) 6908.
- [31] F. Scott, C. Krüger, P. Betz, *J. Organomet. Chem.* 387 (1990) 113.
- [32] I. Bach, K.-R. Pörschke, R. Goddard, C. Kopiske, C. Krüger, A. Rufinska, K. Seevogel, *Organometallics* 15 (1996) 4959.
- [33] S.V. Lindeman, T. Mori, J.K. Kochi, Electronic submission to the Cambridge Structural Database 138879, 2000.
- [34] H. Chen, R.A. Bartlett, M.M. Olmstead, P.P. Power, S.C. Shoner, *J. Am. Chem. Soc.* 112 (1990) 1048.
- [35] J. Terheijden, G. van Koten, I.C. Vinke, A.L. Spek, *J. Am. Chem. Soc.* 107 (1985) 2891.
- [36] M. Mascal, J. Hansen, A.J. Blake, W.-S. Li, *Chem. Commun.* (1998) 355.
- [37] A.S. Batsanov, S.P. Crabtree, J.A.K. Howard, C.W. Lehmann, M. Kilner, *J. Organomet. Chem.* 550 (1998) 59.
- [38] J.B. Lambert, S. Zhang, S.M. Ciro, *Organometallics* 13 (1994) 2430.
- [39] G.S. Hair, A.H. Coley, R.A. Jones, B.G. McBurnett, A. Voigt, *J. Am. Chem. Soc.* 121 (1999) 4922.
- [40] S.V. Lindeman, T. Dhanasekaran, J.K. Kochi, Electronic submission to the Cambridge Structural Database 138880, 2000.
- [41] R. Rathore, J. Hecht, J.K. Kochi, *J. Am. Chem. Soc.* 120 (1998) 13278.
- [42] W. Lau, J.C. Huffman, J.K. Kochi, *J. Am. Chem. Soc.* 104 (1982) 5515.
- [43] C.L. Higgitt, A.H. Klahn, M.H. Moore, B. Oelckers, M.G. Partridge, R.N. Perutz, *J. Chem. Soc. Dalton Trans.* (1997) 1269.



- [44] I.L. Fedushkin, M.N. Bochkarev, H. Schumann, L. Esser, G. Kociok-Köhn, J. Organomet. Chem. 489 (1995) 145.
- [45] M. Jang, J.E. Ellis, Angew. Chem. Int. Ed. Engl. 33 (1994) 1973.
- [46] A.S. Batsanov, Y.T. Struchkov, G.P. Zol'nikova, I.I. Kritskaya, D.N. Kravtsov, Dokl. Akad. Nauk. SSSR 293 (1987) 614.
- [47] H.-F. Klein, K. Ellrich, S. Lamac, G. Lull, L. Zsolnai, G. Hutter, Z. Naturforsch. Teil B 40 (1985) 1377.
- [48] R. Boese, A. Stanger, P. Stellberg, A. Shazar, Angew. Chem. Int. Ed. Engl. 32 (1993) 1475.
- [49] P.A. Wexler, D.E. Wigley, J.B. Koerner, T.A. Albright, Organometallics 10 (1991) 2319.
- [50] D.S. Arney, P.A. Fox, M.A. Bruck, D.E. Wigley, Organometallics 16 (1997) 3421.
- [51] S.V. Lindeman, T. Mori, J.K. Kochi, Electronic submission to the Cambridge Structural Database 138881, 2000.
- [52] S.V. Lindeman, T. Mori, J.K. Kochi, Electronic submission to the Cambridge Structural Database 138882, 2000.
- [53] H. Schmidbaur, U. Thewalt, T. Zafiropoulos, Organometallics 2 (1983) 1550.
- [54] U. Thewalt, T. Zafiropoulos, H. Schmidbaur, Z. Naturforsch. Teil B 39 (1984) 1642.
- [55] D.L. Clark, J.C. Gordon, J.T. McFarlan, R.-L. Vincent-Mollis, J.G. Watkin, B.D. Zwick, Inorg. Chim. Acta 244 (1996) 269.
- [56] F. Calderazzo, F. Gingl, G. Pampaloni, L. Rocchi, J. Strahle, Chem. Ber. 125 (1992) 1005.
- [57] A.L. Spek, A.J.M. Duisenberg, Cryst. Struct. Commun. 10 (1981) 1531.
- [58] F. Jellinek, J. Organomet. Chem. 1 (1963) 43.
- [59] U. Beck, W. Hummel, H.-B. Burgi, A. Ludi, Organometallics 6 (1987) 20.
- [60] A.J. Blake, P.J. Dysen, R.O. Gould, B.F.G. Johnson, S. Parsons, Acta Crystallogr. Sect. C 51 (1995) 582.
- [61] T.W. Bell, M. Helliwell, M.G. Partridge, R.N. Perutz, Organometallics 11 (1992) 1911.
- [62] J. Müller, T. Akhnouk, P.E. Gaede, A. Guo, P. Moran, K. Qiao, J. Organomet. Chem. 54 (1997) 207.
- [63] C. Bianchini, K.G. Caulton, C. Chardon, O. Eisenstein, K. Folting, T.J. Johnson, A. Meli, M. Peruzzini, D.J. Rauscher, W.E. Streib, F. Vizza, J. Am. Chem. Soc. 113 (1991) 5127.
- [64] C.A. Reed, Acc. Chem. Res. 31 (1998) 133.
- [65] A. Bondi, J. Phys. Chem. 68 (1964) 441.
- [66] (a) R.E. Lehmann, J.K. Kochi, J. Am. Chem. Soc. 113 (1991) 501. (b) See also: D. Astruc, Synlett (1991) 369.
- [67] J. Chatt, J.M. Davidson, J. Chem. Soc. (1965) 843.
- [68] S.D. Ibekwe, B.T. Kilbourn, U.A. Raeburn, D.R. Russell, J. Chem. Soc. A (1997) 1118.
- [69] G.W. Parshall, Acc. Chem. Res. 8 (1975) 113.
- [70] W.A. Gustavson, P.S. Epstein, M.D. Curtis, Organometallics 1 (1982) 884.
- [71] Y. Fujiwara, T. Kawauchi, H. Taniguchi, J. Chem. Soc. Chem. Commun. (1980) 220.
- [72] W.D. Jones, F.J. Feher, Organometallics 2 (1983) 686.
- [73] (a) D.F. McMillen, D.M. Golden, Annu. Rev. Phys. Chem. 33 (1982) 493. (b) See also: R.C. Weast (Ed.), CRC Handbook of Chemistry and Physics, 70th ed., CRC Press, Boca Raton, FL, 1989, p. 206.
- [74] W.D. Jones, F.J. Feher, J. Am. Chem. Soc. 104 (1982) 4240.
- [75] W.D. Jones, F.J. Feher, J. Am. Chem. Soc. 106 (1984) 1650.
- [76] J. Sweet, W.A.G. Graham, J. Am. Chem. Soc. 105 (1983) 305.
- [77] R.M. Chin, L. Dong, S.B. Duckett, M.G. Partridge, W.D. Jones, R.N. Perutz, J. Am. Chem. Soc. 115 (1993) 7685.
- [78] P. Diversi, S. Iacoponi, G. Ingrosso, F. Laschi, A. Luccherini, C. Pinzini, G. Uccello-Barretta, P. Zanello, Organometallics 14 (1995) 3275.
- [79] See ref. [5] and references therein.
- [80] G. Jaouen, Ann. N.Y. Acad. Sci. 295 (1977) 59.
- [81] W.S. Trahanovski, R.J. Card, J. Am. Chem. Soc. 94 (1972) 2897.
- [82] A. Cecon, A. Gambaro, A. Venzo, J. Organomet. Chem. 275 (1984) 209.
- [83] J. Lebib, J. Brocard, D. Couturier, Bull. Soc. Chim. Fr. Part II (1982) 357.

- [84] M.-C. Sénéchal-Tocquer, D. Sénéchal, J.-Y. LeBihan, D. Gentric, B. Caro, *J. Organomet. Chem.* 291 (1985) C5.
- [85] R.D. Pike, D.A. Sweigart, *Coord. Chem. Rev.* 187 (1999) 183.
- [86] F. Moulines, F. Gloaguen, D. Astruc, *Angew. Chem. Int. Ed. Engl.* 32 (1992) 458.
- [87] J.-L. Fillaut, D. Astruc, *New J. Chem.* 20 (1996) 945.
- [88] C. Valerio, B. Gloaguen, J.-L. Fillaut, D. Astruc, *Bull. Soc. Chim. Fr.* 133 (1996) 101.
- [89] S.P. Kolis, M.E. Kopach, R. Liu, W.D. Harman, *J. Am. Chem. Soc.* 120 (1998) 6205.
- [90] J.M. Masnovi, S. Sankararaman, J.K. Kochi, *J. Am. Chem. Soc.* 111 (1989) 2263.
- [91] V.D. Parker, Y. Zhao, Y. Lu, G. Zheng, *J. Am. Chem. Soc.* 120 (1998) 12720.
- [92] E.I. Heiba, R.M. Dessau, W.J. Koehl Jr., *J. Am. Chem. Soc.* 91 (1969) 6830.
- [93] A.E. Shilov, *Activation of Saturated Hydrocarbons by Transition Metal Complexes*, Reidel, Dordrecht, 1984, p. 21.
- [94] R. Taylor, *Electrophilic Aromatic Substitution*, Wiley, New York, 1990.
- [95] J. March, *Advanced Organic Chemistry*, Wiley, New York, 1992, p. 641, and references therein.
- [96] S. Sun, C.A. Dullaghan, D.A. Sweigart, *J. Chem. Soc. Dalton Trans.* (1996) 4493.
- [97] M.F. Semmelhack, in: E.W. Abel, F.G.A. Stone, G. Wilkinson (Eds.), *Comprehensive Organometallic Chemistry II*, vol. 12, Pergamon, Oxford, 1995, p. 979.
- [98] V.D. Parker, *Acc. Chem. Res.* 17 (1984) 243.
- [99] B. Reitsch, V.D. Parker, *J. Am. Chem. Soc.* 113 (1991) 6954.
- [100] F. Norrissell, K.L. Handoo, V.D. Parker, *J. Org. Chem.* 58 (1993) 4929.
- [101] J.F. Evans, H.N. Blount, *J. Org. Chem.* 41 (1976) 516.
- [102] L.J. Johnston, N.P. Schepp, in: P.S. Mariano (Ed.), *Advances in Electron Transfer Chemistry*, vol. 5, JAI Press, London, 1996, p. 41.
- [103] D. Astruc, *Tetrahedron* 39 (1983) 4027.
- [104] R.M. Moriarty, U.S. Gill, Y.Y. Ku, *J. Organomet. Chem.* 350 (1988) 157.
- [105] A.S. Abd-El-Aziz, C.R. de Denu, *J. Chem. Soc. Perkin Trans. I* (1993) 293.
- [106] R.L. Chowdhury, C.C. Lee, A. Piórko, R.G. Sutherland, *Synth. React. Inorg. Met. Org. Chem.* 15 (1985) 1237.
- [107] C.C. Lee, A.S. Abd-El-Aziz, R.L. Chowdhury, A. Piórko, R.G. Sutherland, *Synth. React. Inorg. Met. Org. Chem.* 16 (1986) 541.
- [108] A.S. Abd-El-Aziz, C.C. Lee, A. Piórko, R.G. Sutherland, *J. Organomet. Chem.* 348 (1988) 95.
- [109] R.G. Sutherland, R.L. Chowdhury, A. Piórko, C.C. Lee, *Can. J. Chem.* 64 (1986) 2031.
- [110] R.C. Cambie, S.J. Janssen, P.S. Rutledge, P.D. Woodgate, *J. Organomet. Chem.* 434 (1992) 97.
- [111] R.M. Moriarty, U.S. Gill, *Organometallics* 5 (1986) 253.
- [112] A. Ceccon, A. Gambaro, F. Gottardi, R. Manoli, A. Venzo, *J. Organomet. Chem.* 363 (1989) 91.
- [113] M. Perez, P. Potier, S. Halazy, *Tetrahedron Lett.* 37 (1996) 8487.
- [114] J.P. Gilday, D.A. Widdowson, *Tetrahedron Lett.* 27 (1986) 5525.
- [115] M.J. Dickens, J.P. Gilday, T.J. Mowlem, D.A. Widdowson, *Tetrahedron* 47 (1991) 8621.
- [116] A. Alemagna, P. Cremonesi, P. del Buttero, E. Licandro, S. Maiorana, *J. Org. Chem.* 48 (1983) 3114.
- [117] J.A. Heppert, M.E. Thomas-Miller, P.N. Swepston, M.W. Extine, *J. Chem. Soc. Chem. Commun.* (1988) 280.
- [118] J.A. Heppert, M.E. Thomas-Miller, D.M. Scherubel, F. Takusagawa, M.A. Morgenstern, M.R. Shaker, *Organometallics* 8 (1989) 1199.
- [119] P.L. Pauson, J.A. Segal, *J. Chem. Soc. Dalton Trans.* (1975) 1677.
- [120] Y.K. Chung, P.G. Williard, D.A. Sweigart, *Organometallics* 1 (1982) 1053.
- [121] P.J.C. Walker, R.J. Mawby, *J. Chem. Soc. Dalton Trans.* (1973) 622.
- [122] F.A. Cotton, *J. Am. Chem. Soc.* 90 (1968) 6230.
- [123] D.J. Brauer, C. Kruger, *Inorg. Chem.* 16 (1977) 884.
- [124] A. Streitwieser, *Molecular Orbital Theory for Organic Chemists*, Wiley, New York, 1961, p. 246.
- [125] W.L. Jorgensen, L. Salem, *The Organic Chemist's Book of Orbitals*, Academic Press, New York, 1973, p. 257.
- [126] L.R. Falvello, J. Forniés, R. Navarro, V. Sicilia, M. Tomás, *J. Chem. Soc. Dalton Trans.* (1994) 3143.

- [127] J. Forniés, B. Menjón, N. Gómez, M. Tomás, *Organometallics* 11 (1992) 1187.
- [128] D.R. Neithamer, L. Párkányi, J.F. Mitchell, P.T. Wolczanski, *J. Am. Chem. Soc.* 110 (1988) 4421.
- [129] G.A. Olah, H.C. Lin, Y.K. Mo, *J. Am. Chem. Soc.* 94 (1972) 3667.
- [130] R. Uson, A. Laguna, A. Uson, P.G. Jones, K. Meyer-Base, *J. Chem. Soc. Dalton Trans.* (1988) 341.
- [131] G. Boche, F. Basold, M. Marsch, K. Harms, *Angew. Chem. Int. Ed. Engl.* 37 (1998) 1684.
- [132] A.G. Orpen, L. Brammer, F.H. Allen, O. Kennard, D.G. Watson, R. Taylor, *J. Chem. Soc. Dalton Trans.* (1989) S1.
- [133] M.R. Mason, J.M. Smith, S.G. Bott, A.R. Barron, *J. Am. Chem. Soc.* 115 (1993) 4971.
- [134] R.A. Bartlett, H. Chen, P.P. Power, *Angew. Chem. Int. Ed. Engl.* 28 (1989) 316.
- [135] S.V. Lindeman, T. Dhanasekaran, J.K. Kochi, Electronic submission to the Cambridge Structural Database 138883, 2000.
- [136] S.V. Lindeman, T. Dhanasekaran, J.K. Kochi, Electronic submission to the Cambridge Structural Database 138884, 2000.
- [137] P.G. Jones, D. Henschel, A. Weitze, A. Blaschette, *Z. Anorg. Allg. Chem.* 620 (1994) 1514.
- [138] W.A. Kiel, G.-Y. Lin, A.G. Constable, F.B. McCermick, C.E. Strouse, O. Eisenstein, J.A. Gladys, *J. Am. Chem. Soc.* 104 (1982) 4865.
- [139] H. van der Heijen, A.G. Orpen, P. Pasman, *J. Chem. Soc. Chem. Commun.* (1985) 1576.
- [140] W.D. Harman, D.P. Fairlie, H. Taube, *J. Am. Chem. Soc.* 108 (1986) 8223.
- [141] W.D. Harman, M. Gebhard, H. Taube, *Inorg. Chem.* 29 (1990) 567.
- [142] S.T. Belt, S.B. Duckett, M. Helliwell, R.N. Perutz, *J. Chem. Soc. Chem. Commun.* (1989) 928.
- [143] C.P. Brock, J.D. Dunitz, *Acta Crystallogr. Sect. B* 38 (1982) 2218.
- [144] C.P. Brock, J.D. Dunitz, *Acta Crystallogr. Sect. B* 46 (1990) 795.
- [145] R.M. Chin, L. Dong, S.B. Duckett, W.D. Jones, *Organometallics* 11 (1992) 871.